

**CONVERSION OF *n*-PENTANE TO LIGHT OLEFINS OVER MODIFIED
Zr/HZSM-5-BASED CATALYSTS**

Bharanabha Makkaron

A Thesis Submitted in Partial Fulfillment of the Requirements
for the Degree of Master of Science
The Petroleum and Petrochemical College, Chulalongkorn University
in Academic Partnership with
The University of Michigan, The University of Oklahoma,
Case Western Reserve University, and Institut Français du Pétrole
2020

บทคัดย่อและแฟ้มข้อมูลฉบับเต็มของวิทยานิพนธ์ตั้งแต่ปีการศึกษา 2554 ที่ให้บริการในคลังปัญญาจุฬาฯ (CUIR)
เป็นแฟ้มข้อมูลของนิสิตเจ้าของวิทยานิพนธ์ที่ส่งผ่านทางบัณฑิตวิทยาลัย



The abstract and full text of theses from the academic year 2011 in Chulalongkorn University Intellectual Repository (CUIR)
are the thesis authors' files submitted through the Graduate School.

Conversion of *n*-Pentane to Light Olefins over Modified Zr/HZSM-5-based Catalysts

Miss Bharanabha Makkaron

A Thesis Submitted in Partial Fulfillment of the Requirements
for the Degree of Master of Science in Petrochemical Technology
Common Course
the Petroleum and Petrochemical College
Chulalongkorn University
Academic Year 2019
Copyright of Chulalongkorn University

2420444977
CD IThesis 6171002063 thesis / recv: 31072563 03:53:59 / seq: 17

การเปลี่ยนสภาพสารนอร์มัลเพนเทนให้เป็นโอเลฟินส์เบาโดยตัวเร่งปฏิกิริยาเซอร์โคเนียมบนตัว
รองรับเอชแซดเอสเอ็ม-5 ที่ปรับปรุงคุณภาพ

น.ส.ภรณา มัถการุณ

วิทยานิพนธ์นี้เป็นส่วนหนึ่งของการศึกษาตามหลักสูตรปริญญาวิทยาศาสตรมหาบัณฑิต
สาขาวิชาเทคโนโลยีปิโตรเคมี ไม่สังกัดภาควิชา/...
วิทยาลัยปิโตรเลียมและปิโตรเคมี จุฬาลงกรณ์มหาวิทยาลัย
ปีการศึกษา 2562
ลิขสิทธิ์ของจุฬาลงกรณ์มหาวิทยาลัย

Thesis Title Conversion of *n*-Pentane to Light Olefins over Modified
Zr/HZSM-5-based Catalysts
By Miss Bharanabha Makkaroon
Field of Study Petrochemical Technology
Thesis Advisor Associate Professor SIRIPORN JONGPATIWUT,
Ph.D.

Accepted by the the Petroleum and Petrochemical College, Chulalongkorn
University in Partial Fulfillment of the Requirement for the Master of Science

..... Dean of the the Petroleum and
Petrochemical College
(Professor SUWABUN CHIRACHANCHAI, Ph.D.)

THESIS COMMITTEE

..... Chairman
(Professor APANEE LUENGNARUEMITCHAI, Ph.D.)

..... Thesis Advisor
(Associate Professor SIRIPORN JONGPATIWUT,
Ph.D.)

..... External Examiner
(Assistant Professor Sitthiphong Pengpanich, Ph.D.)

GRAPHICAL ABSTRACT



242044977

CU IThesis 6171002063 thesis / revv: 31072563 03:53:59 / seq: 17

ภรณา มัถการุณ : การเปลี่ยนสภาพสารนอร์มัลเพนเทนให้เป็นโอเลฟินส์เบาโดย
ตัวเร่งปฏิกิริยาเซอร์โคเนียมบนตัวรองรับเอชแซดเอสเอ็ม-5 ที่ปรับปรุงคุณภาพ. (
Conversion of *n*-Pentane to Light Olefins over Modified
Zr/HZSM-5-based Catalysts) อ.ที่ปรึกษาหลัก : รศ. ดร.ศิริพร จง
ผาติวุฒิ

เอทิลีนและโพรพิลีนเป็นสารตั้งต้นที่สำคัญในการผลิตสารเคมีและพอลิเมอร์หลากหลายชนิด เมื่อไม่นานมานี้ความต้องการซื้อของโพรพิลีนมีมากขึ้นส่งผลให้ความต้องการในอัตราส่วนการผลิตโพรพิลีนต่อเอทิลีนเพิ่มเป็น 0.85 และเพื่อเพิ่มการผลิตโพรพิลีนให้บรรลุเป้าหมายดังกล่าว การพัฒนาตัวเร่งปฏิกิริยาเอชแซดเอสเอ็ม-5 แบบผสมสำหรับกระบวนการแตกตัวโมเลกุลโดยใช้ตัวเร่งปฏิกิริยาหลายเป็นที่น่าสนใจมากขึ้น ความสามารถในการทำให้แตกตัวจากความเป็นกรดของซีโอไลต์เอชแซดเอสเอ็ม-5 และการบรรจุโลหะลงบนเอชแซดเอสเอ็ม-5 เพื่อปรับปรุงคุณสมบัติของตัวเร่งปฏิกิริยาคาดว่าจะสามารถส่งเสริมความว่องไวในการเกิดปฏิกิริยาดีไฮโดรจิเนชันซึ่งน่าจะช่วยเพิ่มอัตราส่วนการผลิตโพรพิลีนต่อเอทิลีน หนึ่งในสารตั้งต้นที่น่าสนใจสำหรับกระบวนการนี้คือนอร์มอลเพนเทนซึ่งเป็นผลิตภัณฑ์มูลค่าต่ำจากกระบวนการกลั่นน้ำมัน ตัวเร่งปฏิกิริยาที่มีการศึกษาอย่างมากในปฏิกิริยาการแตกตัวของนอร์มัลเพนเทนคือ ตัวเร่งปฏิกิริยาเซอร์โคเนียมบนเอชแซดเอสเอ็ม-5 ซึ่งสามารถให้ความว่องไวและเสถียรภาพที่ดีสำหรับปฏิกิริยานี้ งานวิจัยนี้แบ่งออกเป็นสองส่วน ส่วนแรกคือการศึกษาผลของโลหะตัวที่สองคือ แพลเลเดียม, นิกเกิล และเงิน บนตัวเร่งปฏิกิริยาเซอร์โคเนียมบนเอชแซดเอสเอ็ม-5 พบว่า ตัวเร่งปฏิกิริยาเงินและเซอร์โคเนียมบนเอชแซดเอสเอ็ม-5 แสดงถึงความว่องไวในการดีไฮโดรจิเนชันและการแตกตัวดีที่สุด โดยสังเกตได้จากอัตราส่วนโพรพิลีนต่อเอทิลีนที่สูงที่สุด (0.89) เมื่อเทียบกับผลที่ได้จากตัวเร่งปฏิกิริยาอื่น ซึ่งเป็นผลจากความเป็นกรดของตัวเร่งปฏิกิริยาโดยเงินและเซอร์โคเนียมบนเอชแซดเอสเอ็ม-5 มีความเป็นกรดต่ำที่สุด ส่วนที่สองคือการศึกษาผลของอัตราส่วนซิลิกา-อะลูมินา 23, 50 และ 80 ในตัวเร่งปฏิกิริยาเงินและเซอร์โคเนียมบนเอชแซดเอสเอ็ม-5 พบว่าเงินและเซอร์โคเนียมบนเอชแซดเอสเอ็ม-5 จากอัตราส่วนซิลิกา-อะลูมินา 80 มีความเป็นกรดต่ำที่สุด ส่งผลให้ได้อัตราส่วนโพรพิลีนต่อเอทิลีนสูงที่สุด (1.25) แต่ให้เสถียรภาพต่ำ สามารถสรุปได้ว่าตัวเร่งปฏิกิริยาที่มีความเป็นกรดที่เหมาะสมนั้นเหมาะสำหรับปฏิกิริยาการแตกตัวของนอร์มอลเพนเทนเพื่อเพิ่มความจำเพาะเจาะจงต่อโพรพิลีน

สาขาวิชา เทคโนโลยีปิโตรเคมี

ลายมือชื่อนิลิต

ปีการศึกษา 2562

ลายมือชื่อ อ.ที่ปรึกษาหลัก

6171002063 : MAJOR PETROCHEMICAL TECHNOLOGY

KEYWORD n-Pentane/ Propylene/ Ethylene/ Catalytic cracking/ Light olefins
D:

Bharanabha Makkaroon : Conversion of *n*-Pentane to Light Olefins over Modified Zr/HZSM-5-based Catalysts. Advisor: Assoc. Prof. SIRIPORN JONGPATIWUT, Ph.D.

Ethylene and propylene are important raw materials for producing several types of chemicals and polymers. According to the increase of propylene demand in recent year, the P/E ratio was increased to 0.85. In order to meet the propylene demand, the development of hybrid HZSM-5 catalyst for catalytic cracking becomes more interesting owing to the cracking activity from HZSM-5 zeolite acid site and loaded metal on HZSM-5 that expected to promote the dehydrogenation activity to the catalyst which could possibly enhanced the P/E ratio. The alternative feedstock for this process is *n*-pentane which is the low-value product from distillation process. The most studied catalyst in *n*-pentane catalytic cracking is based on Zr/HZSM-5 which provides a good activity and stability. This work was divided into two major parts. In the first part, the effect of second metal Pd, Ni and Ag on Zr/HZSM-5 catalysts were studied. It was found that AgZr/HZSM-5 catalysts exhibited the best dehydrogenation and cracking activity that can be observed from highest P/E ratio (0.89) when compared to the effect from other second metals, related to the acidity of catalysts that AgZr/HZSM-5 showed the lowest acidity. In the second part, the effect of SiO₂/Al₂O₃ ratios (23, 50 and 80) in AgZr/HZSM-5 catalysts were studied. It was found that AgZr/HZSM-5 (80) shows the lowest acidity, resulting in the highest P/E ratio (1.25) but poor stability. In conclusion, the appropriated low acidity catalyst convenient for *n*-pentane catalytic cracking in order to enhance propylene selectivity.

Field of Study:	Petrochemical Technology	Student's Signature
Academic Year:	2019 Advisor's Signature

ACKNOWLEDGEMENTS

I would like to express my deep special thanks to my thesis advisor, Assoc.Prof. Siriporn Jongpatiwut who gave me a valuable opportunity to do this project and also supported me to overcome a lot of problems in this project.

My sincere thanks also go to the thesis committees, Prof. Apanee Luengnaruemitchai and Dr. Sitthiphong Pengpanich for their comments and suggestions.

I am particularly grateful for the partial scholarship and partial funding of the thesis work provided by the Petroleum and Petrochemical College and Center of Excellence on Petrochemical and Materials Technology (PETROMAT).

I wish to acknowledge the help provided by my family, friends and all members in the SP group.

Lastly, my special thanks are extended to all PPC friends and staff for their support and help in many occasions.

Bharanabha Makkaroon

TABLE OF CONTENTS

	Page
ABSTRACT (THAI)	iii
ABSTRACT (ENGLISH).....	iv
ACKNOWLEDGEMENTS.....	v
TABLE OF CONTENTS.....	vi
LIST OF TABLES	ix
LIST OF FIGURES	x
CHAPTER 1 INTRODUCTION	1
CHAPTER 2 LITERATURE REVIEW	3
2.1 Light Olefins	4
2.2 Naphtha Feedstock.....	6
2.2.1 <i>n</i> -Pentane.....	7
2.3 Catalytic Cracking of Light Alkanes	8
2.3.1 Zeolite Material	8
2.3.1.1 Zeolite Structure	8
2.3.1.2 Zeolite Types.....	10
2.3.1.3 Zeolites as Supports.....	11
2.3.1.4 Possible Reaction Pathways for <i>n</i> Pentane Cracking.....	12
2.3.1.5 Deactivation of Catalyst	14
2.4 Modification of Zeolite.....	14
2.4.1 Metal Incorporation.....	14
CHAPTER 3 EXPERIMENTAL.....	17
3.1 Catalyst Preparation.....	18
3.1.1 Incipient Wetness Impregnation.....	18

3.1.2 Catalytic Activity Testing	19
3.1.3 Catalyst Characterization	20
3.1.3.1 Temperature Programmed Reduction of Hydrogen (H ₂ -TPR).....	20
3.1.3.2 Temperature Programmed Oxidation (TPO)	20
3.1.3.3 Temperature Programmed Desorption (TPD) of Ammonia	20
3.1.3.4 X-ray Fluorescence Spectroscopy (XRF)	20
3.1.3.5 N ₂ Adsorption/Desorption Measurement	21
3.1.3.6 X-ray Diffraction (XRD)	21
3.1.3.7 Leco CHNS Elemental Analyzer	22
3.1.3.8 Transmission Electron Microscope (TEM)	22
CHAPTER 4 RESULTS AND DISCUSSION	23
4.1 Catalyst Characterization	23
4.1.1 X-ray Diffraction	23
4.1.2 Brunauer–Emmett–Teller (BET) Surface Analyzer and X-ray Fluorescence Spectrometer (XRF)	24
4.1.3 Transmission Electron Microscope (TEM)	25
4.1.4 Temperature Programmed Desorption of Ammonia (NH ₃ -TPD)	27
4.1.5 Temperature Programmed Reduction of Hydrogen (H ₂ -TPR).....	29
4.1.6 Temperature Programmed Oxidation (TPO) and CHNS/O Analyzer	30
4.2 Catalytic Activity Testing	32
4.2.1 Effect of Second Metals Loading	32
4.2.2 Effect of HZSM-5 Zeolites SiO ₂ /Al ₂ O ₃ Ratio	35
4.2.2.1 Effect of Weight Hourly Space Velocity (WHSV)	38
4.3 Catalytic Stability	40
4.3.1 Effect of Second Metal Loadings	40
4.3.2 Effect of SiO ₂ /Al ₂ O ₃ Ratios	43

CHAPTER 5 CONCLUSIONS AND RECOMMENDATIONS 47

 5.1 Conclusions..... 47

 5.2 Recommendations..... 48

APPENDICES 49

 Appendix A Calculation of Activity Testing..... 49

REFERENCES 50

VITA..... 54

LIST OF TABLES

	Page
Table 2.1 Physical properties of n-pentane	7
Table 2.2 Properties of major synthetic zeolites	11
Table 2.3 Possible reaction pathways for n-pentane cracking over zeolites	13
Table 4.1 The textural properties and element composition of catalysts	25
Table 4.2 The total acid amount of HZSM-5 and modified HZSM-5 catalysts, detected by NH ₃ -TPD	29
Table 4.3 Amount of carbon deposits on HZSM-5 and modified HZSM-5 catalysts after reaction	32

LIST OF FIGURES

	Page
Figure 2.1 North America's olefin production from steam cracker.(Plotkin, 2015). Index 1.0 = North America's olefin production from steam crackers in 2010.	4
Figure 2.2 The growing gap between propylene supply and demand. where MTA = million tons per annum.(Plotkin, 2015).	5
Figure 2.3 Three-dimensional structure of n-pentane.	7
Figure 2.4 Silicon/aluminum oxygen tetrahedron.	9
Figure 2.5 Diagrams of elements of the frameworks of (a) the small pore zeolite Rho, (b) the medium-pore zeolite ZSM-5, and (c) the large-pore zeolite Y. Tetrahedral (aluminum and silicon) cations are represented by small black spheres, and oxygens are represented by larger spheres. Oxygens of selected rings that define access to the internal pore systems are highlighted in dark gray.	10
Figure 3.1 Schematic of the experimental set-up for n-pentane cracking.	19
Figure 4.1 XRD patterns of (a) HZSM-5, (b) 3Zr/HZSM-5, (c) 1.5Ag1.5Zr/HZSM-5, (d) 1.5Pd1.5Zr/HZSM-5 and (e) 1.5Ni1.5Zr/HZSM-5 with SiO ₂ /Al ₂ O ₃ ratio 23.	23
Figure 4.2 XRD patterns of (f) 1.5Ag1.5Zr/HZSM-5 (23), (g) 1.5Ag1.5Zr/HZSM-5 (50) and (h) 1.5Ag1.5Zr/HZSM-5 (80).	24
Figure 4.3 TEM images of calcined (a) parent HZSM-5, (b) 3wt%Zr/HZSM-5, (c) 1.5wt%Pd1.5wt%Zr/HZSM-5, (d) 1.5wt%Ni1.5wt%Zr/HZSM-5, (e) 1.5wt%Ag1.5wt%Zr/HZSM-5 (1) and (f) 1.5wt%Ag1.5wt%Zr/HZSM-5 (2) catalysts.	26
Figure 4.4 NH ₃ -TPD profiles of (a) HZSM-5 (23), (b) 3Zr/HZSM-5 (23), (c) 1.5Pd1.5Zr/HZSM-5 (23), (d) 1.5Ni1.5Zr/HZSM-5 (23), (e) 1.5Ag1.5Zr/HZSM-5 (23), (f) 1.5Ag1.5Zr/HZSM-5 (50) and (g) 1.5Ag1.5Zr/HZSM-5 (80).	28
Figure 4.5 H ₂ -TPR profiles of (a) HZSM-5 (23), (b) 3Zr/HZSM-5 (23), (c) 1.5Pd1.5Zr/HZSM-5 (23), (d) 1.5Ni1.5Zr/HZSM-5 (23), (e) 1.5Ag1.5Zr/HZSM-5 (23), (f) 1.5Ag1.5Zr/HZSM-5 (50) and (g) 1.5Ag1.5Zr/HZSM-5 (80).	30
Figure 4.6 TPO profiles of (a) HZSM-5 (23), (b) 3Zr/HZSM-5 (23), (c) 1.5Pd1.5Zr/HZSM-5 (23), (d) 1.5Ni1.5Zr/HZSM-5 (23), (e) 1.5Ag1.5Zr/HZSM-5 (23), (f) 1.5Ag1.5Zr/HZSM-5 (50) and (g) 1.5Ag1.5Zr/HZSM-5 (80).	31
Figure 4.7 Products distribution from HZSM-5 and modified HZSM-5 catalysts.	34
Figure 4.8 Products yield of light olefins and light paraffins from HZSM-5 and modified HZSM-5 catalysts.	34

Figure 4.9 Ethylene selectivity, propylene selectivity and propylene to ethylene ratio from HZSM-5 and modified HZSM-5 catalysts.....	35
Figure 4.10 Products distribution from 1.5Ag1.5Zr/HZSM-5 catalysts with different SiO ₂ /Al ₂ O ₃ ratios.....	36
Figure 4.11 Products yield of light olefins and light paraffins from 1.5Ag1.5Zr/HZSM-5 catalysts with different SiO ₂ /Al ₂ O ₃ ratios.....	37
Figure 4.12 Ethylene selectivity, propylene selectivity and propylene to ethylene ratio from 1.5Ag1.5Zr/HZSM-5 catalysts with different SiO ₂ /Al ₂ O ₃ ratios.....	38
Figure 4.13 Effect of WHSV on conversion and product distribution from 1.5Ag1.5Zr/HZSM-5 catalyst with SiO ₂ /Al ₂ O ₃ ratio of 80 at TOS 3 h.....	39
Figure 4.14 Effect of WHSV on ethylene, propylene selectivity and propylene to ethylene ratio from 1.5Ag1.5Zr/HZSM-5 catalyst with SiO ₂ /Al ₂ O ₃ ratio of 80 at TOS 3 h.....	39
Figure 4.15 Conversion of n-pentane over HZSM-5 and modified HZSM-5 catalysts at 550 °C, atm, WHSV of 5 h ⁻¹ as a function of time on stream (TOS).	40
Figure 4.16 Light olefins selectivity over HZSM-5 and modified HZSM-5 catalysts at 550 °C, atm, WHSV of 5 h ⁻¹ as a function of time on stream (TOS).....	41
Figure 4.17 Ethylene selectivity of HZSM-5 and modified HZSM-5 catalysts at 550 °C, atm, WHSV of 5 h ⁻¹ as a function of time on stream (TOS).	42
Figure 4.18 Propylene selectivity of HZSM-5 and modified HZSM-5 catalysts at 550 °C, atm, WHSV of 5 h ⁻¹ as a function of time on stream (TOS).	42
Figure 4.19 Conversion of n-pentane over 1.5Ag1.5Zr/HZSM-5 catalysts with different SiO ₂ /Al ₂ O ₃ ratios at 550 °C, atm, WHSV of 5 h ⁻¹ as a function of time on stream (TOS).....	43
Figure 4.20 Light olefins selectivity of 1.5Ag1.5Zr/HZSM-5 catalysts with different SiO ₂ /Al ₂ O ₃ ratios at 550 °C, atm, WHSV of 5 h ⁻¹ as a function of time on stream (TOS).	44
Figure 4.21 Ethylene selectivity of 1.5Ag1.5Zr/HZSM-5 catalysts with different SiO ₂ /Al ₂ O ₃ ratios at 550 °C, atm, WHSV of 5 h ⁻¹ as a function of time on stream (TOS).	45
Figure 4.22 Propylene selectivity of 1.5Ag1.5Zr/HZSM-5 catalysts with different SiO ₂ /Al ₂ O ₃ ratios at 550 °C, atm, WHSV of 5 h ⁻¹ as a function of time on stream (TOS).	46

CHAPTER 1

INTRODUCTION

The conversion of low value light alkanes such as *n*-pentane to be more value-added products is important in the petrochemical industry. Nowadays, the interesting high value-added products are light olefins, especially, ethylene and propylene, which are sometimes called king and crown of chemicals respectively. They are the important building blocks for many petrochemicals products, such as polypropylene, polyethylene, propylene oxide, ethylene oxide, acrylonitrile, cumene, and acrylic acid.(Alotaibi *et al.*, 2018). These building blocks are mainly produced by steam cracking of hydrocarbons such as naphtha. This process requires high amount of energy from high reaction temperature ($> 800\text{ }^{\circ}\text{C}$) which resulted in high amount of CO_2 emission. Moreover, the steam cracking has a limited control over propylene to ethylene ratio.(Haribal *et al.*, 2018).

Catalytic cracking process has gained more attention for light olefins production in recent year because it is not only consuming less energy in production but also inhibits CO_2 emission. Moreover, this process could enhance the propylene to ethylene ratio in order to meet the increase of propylene demand in recent year. (Le Van Mao *et al.*, 2009). The development of high-efficiency HZSM-5 zeolite catalysts has become more considered due to the unique structure and acidity of HZSM-5 zeolites that exhibited excellent activity and stability in naphtha catalytic cracking, reducing reaction temperature and increasing light olefins production.(Usman *et al.*, 2017).

Metal-incorporation is a common method to modify HZSM-5 zeolites. Hou *et al.* (2018) observed the influences of metal-incorporated HZSM-5 zeolite on reaction pathways for *n*-pentane cracking, it was found that the Zr-incorporation of HZSM-5 zeolites improved catalytic activity and stability for the conversion of *n*-pentane at $450\text{--}550\text{ }^{\circ}\text{C}$ in comparison with the parent HZSM-5 catalyst without modification.

In order to enhance the yield and selectivity of ethylene and propylene, we have to introduce dehydrogenation activity to *n*-pentane catalytic cracking by adding the metal that could promote the dehydrogenation activity to the catalyst. Palladium is one of the interesting metals. Zhang *et al.* (2015) developed a palladium (II) catalyst

for dehydrogenation of cyclohexanones to phenols. They found that Pd species served high dehydrogenation rate.

Other interesting metals for promoting dehydrogenation reaction is silver (Ag). Ono and Baba (2015) observed the activation of light alkanes over Ag⁺ - exchanged HZSM-5 zeolite. They reported that Ag⁺ ions significantly enhanced the dehydrogenation of alkanes from its ability of heterolytic dissociation that produced carbenium ion and hydride species.

Moreover, the presence of dehydrogenation site from Ni/HZSM-5 catalyst was investigated. Maia *et al.* (2011) reported that dehydrogenation reaction occurred when the alkane molecule reacts over the nickel site. Therefore, nickel is another interesting metal which is considered lower cost as compared to palladium and silver.

The objective of this work is to study the *n*-pentane catalytic cracking over hybrid catalysts. The incipient wetness impregnation method is used for the catalyst modification in order to obtain monometallic and bimetallic which are Zr/HZSM-5, PdZr/HZSM-5, AgZr/HZSM-5 and NiZr/HZSM-5, respectively. The activity and stability of the prepared catalysts were investigated for the light olefins yield, ethylene selectivity, propylene selectivity, propylene to ethylene molar ratio and coke formation. The XRD, TEM, NH₃-TPD, H₂-TPR, TPO, CHNS Analyzer, XRF and surface area analyzer will be used for catalysts characterization.

CHAPTER 2

LITERATURE REVIEW

Light olefins such as ethylene and propylene play an important role for the petrochemical production. Thermal cracking of naphtha is a main route to produce light olefins. Although 24–55% of ethylene and 1.5-18% of propylene can be obtained by thermal cracking process (Wei *et al.*, 2005). By the way, thermal cracking requires high energy consumption (reaction temperature (>800 °C)) and causes CO₂ emission, which makes it become the first energy-consuming process in the petrochemical industry by consuming nearly 40% of the total energy used by this field. Furthermore, thermal cracking process has a limitation to control product distribution.

In North America and the Middle East, ethane and associate gas already make up 25 - 40% of the feedstock for steam cracking. This causes an imbalance in the ethylene to propylene ratio in the overall output from steam cracking because typical ethane pyrolysis gives 79% selectivity to ethylene and less than 1% selectivity to propylene at 70% conversion, whereas steam cracking of naphtha gives approximately 30% ethylene and 15% propylene. It is predicted that by 2010, the annual demand for ethylene and propylene will be 120 Mt and 82 Mt respectively (a propylene to ethylene ratio of 0.68).

The propylene stream from refineries currently accounts for one third of the total supply, and it is clearly necessary to develop new ways of increasing propylene production. A variety of new processes for modifying the propylene to ethylene ratio are emerging.(Amghizar *et al.*, 2017). Various processes such as dehydrogenation of ethane and propane and catalytic cracking have been received more attention to overcome those limitations. Catalytic cracking has been considered as the most effective method to produce light olefins due to its ability to reduce reaction temperature and control product distribution. One of the interesting feedstocks is *n*-pentane, which is produced as a by-product in the naphtha cracking.



242044977

CU Theses 6171002063 thesis / rev: 31072563 03:53:59 / seq: 17

2.1 Light Olefins

Olefins are considered as a key component of the chemical industry. Ethylene and propylene are the most important olefins, with an annual production of roughly 1.5×10^8 t and 8×10^7 t, respectively. (Zimmermann and Walzl, 2000).

Ethylene (C_2H_4) is used primarily to manufacture polyethylene, ethylene chloride and ethylene oxide. These products are very useful for the packaging, plastic processing, construction and textile industry.

Most propylene (C_3H_6) is used to make polypropylene, but it is also a basic product necessary to produce propylene oxide, acrylic acid and many other chemical derivatives. Not only plastic processing, the packaging industry and the furnishing sector, but also the automotive industry are users of propylene and its derivatives.

However, naphtha crackers will produce the largest fraction of the total ethylene production capacity. Increasing ethane cracking has led to a decline in the production volumes of some co-products such as propylene, as shown in Figure 2.1.

Due to the problem of increasing in demand of propylene, it becomes to develop the new process that can adjust ratio of ethylene to propylene production. It can be expected that catalytic processes will play a significant role in the production of light olefins, especially when heavy or low-grade oil such as *n*-pentane is used as the feedstock.

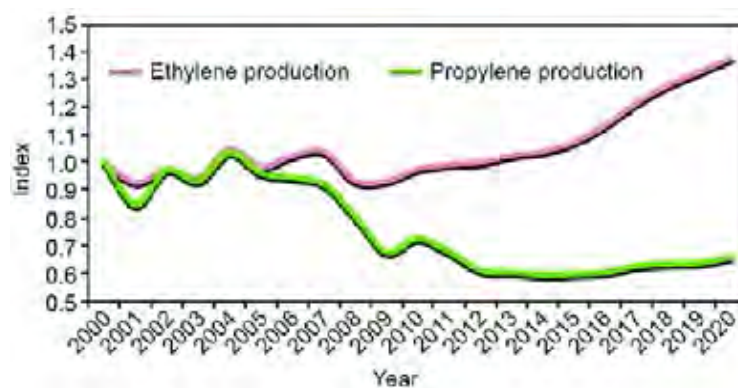


Figure 2.1 North America's olefin production from steam cracker. (Plotkin, 2015). Index 1.0 = North America's olefin production from steam crackers in 2010.

There will be continued growth in worldwide demand for light olefins like ethylene and propylene at a projected 4 percent compound annual growth rate, supporting investment in additional petrochemical facilities.(Kee *et al.*, 2017).

The demand for propylene is mostly from the expanding middle class in developing countries, particularly in China, India, and Southeast Asia. The majority of the demand for propylene will be filled by propane dehydrogenation (PDH) plants in North America and methane-to-olefin (MTO) plants in China, although China is also importing an increasing amount of propane from the United States.

Bricker explained that there is a growing gap in the supply-versus-demand curve for propylene (see Figure 2.2) as a result of two factors: Steam crackers have been shifting to lighter feedstocks that produce less propylene, and flat demand for gasoline in some regions has limited the amount of propylene produced during the oil-refining process. His colleagues at UOP believe that so-called on-purpose propylene will supply one quarter of the world's demand by 2021.

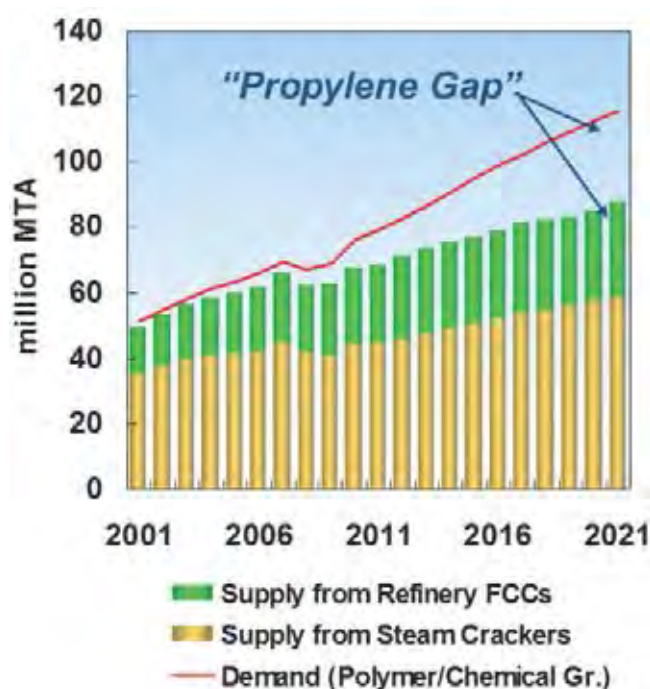


Figure 2.2 The growing gap between propylene supply and demand. where MTA = million tons per annum.(Plotkin, 2015).

2.2 Naphtha Feedstock

Naphtha is an intermediate hydrocarbon liquid stream derived from the refining of crude oil and it can be divided to two types of naphtha. Firstly, light naphtha mostly contains $C_5 - C_6$ with boiling range is 30-145 °C and heavy naphtha contains most of the hydrocarbon with more than 6 carbon atoms which has boiling range about 140-205 °C.

The naphtha feedstock consists of:

Paraffins or alkanes is an acyclic saturated hydrocarbon. It is generally known that alkanes contain only hydrogen and carbon atoms arranged in a tree structure with single bond of carbon-carbon atom. The general chemical formula of alkanes is C_nH_{2n+2} and weakly react with ionic and other polar substances. The paraffin density increases with increasing carbon number.

Olefins or light alkenes is an unsaturated hydrocarbon that contains at least one carbon-carbon double bond. The words alkene, olefin, and olefin are used often interchangeably. The general formula of alkenes is C_nH_{2n} . The physical properties of alkenes and alkanes are similar. The simplest alkenes, ethene, propene, and butene are gas state at room temperature.

Naphthenes or cycloalkanes are saturated cyclic hydrocarbons that contain at least one ring structure. The general formula for mononaphthenes is C_nH_{2n} same as olefins. Five and six carbon atoms are the most abundant cycloalkane in petroleum industry. The rings can have paraffinic side chains attached to them. The boiling point and the density are higher than paraffin at the same number of carbon atoms.

Aromatics contain one or more polyunsaturated rings (conjugated double bonds). These benzene rings can have paraffinic side chains or be coupled with other naphthenic or aromatic rings. The boiling points and the density of these aromatic compounds are higher than both paraffins and naphthenes with the same carbon number.

2.2.1 *n*-Pentane

Pentane is an organic compound with the formula C_5H_{12} . The three-dimensional structure of *n*-pentane is shown in Figure 2.3.

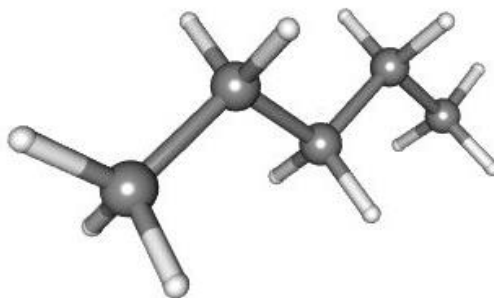


Figure 2.3 Three-dimensional structure of *n*-pentane.

The physical properties of *n*-pentane are shown in Table 2.1.

Table 2.1 Physical properties of *n*-pentane

Molecular weight	72.151 g/mol
Density	0.626 g/ml (at 20 °C)
Boiling point	35.9 to 36.3 °C
Melting point	-130.5 to -129.1 °C
Solubility in water	40 mg/L (at 20 °C)
Vapor pressure	57.90 kPa (at 20.0 °C)

Pentane is relatively inexpensive and are the most volatile liquid alkanes at room temperature, so they are often used in the laboratory as solvents that can be conveniently and rapidly evaporated. However, because of their nonpolarity and lack of functionality, they dissolve only nonpolar and alkyl-rich compounds. Pentanes are miscible with most common nonpolar solvents such as chlorocarbons, aromatics, and ethers.

2.3 Catalytic Cracking of Light Alkanes

Routes for the on-purpose production of light olefins have received more considerable interest. Catalytic cracking provides the possibility of high selectivity to a single olefin product much higher than can be expected from steam cracking alone.

The amount of propylene produced by dehydrogenation was 5×10^6 t in 2014 and is expected to increase, as it has been announced that a dozen new PDH plants (Propane Dehydrogenation Plant) are to be built worldwide. It becomes more challenge for developing the performance catalyst that can give higher selectivity to propylene and higher stability. One of the commonly catalyst that use in catalytic cracking is zeolite.

2.3.1 Zeolite Material

Zeolite is the key ingredient of the FCC catalyst. It provides product selectivity and much of the catalytic activity. The catalyst's performance depends largely on the nature and quality of the zeolite. Understanding the zeolite structure, types, cracking mechanism, and properties is essential in choosing the "right" catalyst to produce the desired yields.

2.3.1.1 *Zeolite Structure*

Zeolite is sometimes called molecular sieve. It has a well-defined lattice structure. Its basic building blocks are silica and alumina tetrahedral (pyramids). Each tetrahedron (Figure 2.4) consists of a silicon or aluminum atom at the center of the tetrahedron, with oxygen atoms at the four corners. Zeolite lattices have a network of very small pores. The pore diameter of nearly all of today's FCC zeolite is approximately 8.0 angstroms (Å). These small openings, with an internal surface area of roughly $600 \text{ m}^2/\text{g}$. The elementary building block of the zeolite crystal is a unit cell. The unit cell size (UCS) is the distance between the repeating cells in the zeolite structure. One-unit cell in a typical fresh Y zeolite lattice contains 192 framework atomic positions: 55 atoms of aluminum and 137 atoms of silicon. This corresponds to a silica (SiO_2) to alumina (Al_2O_3) molal ratio (SAR) of 5. The UCS is an important parameter in characterizing the zeolite structure.

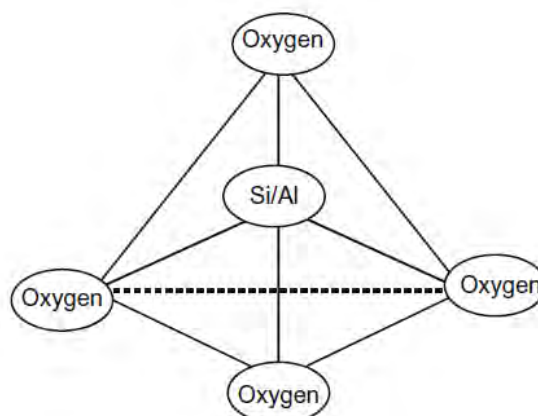


Figure 2.4 Silicon/aluminum oxygen tetrahedron.

Each aluminum atom in the framework introduces a negative charge, which must be balanced by a charge-balancing cation or proton, which can act as a Lewis or Brønsted acid, respectively. The acid forms of zeolites have found wider use as acid catalysts than any other materials. Their outstanding utility derives from their relatively high acid strength, their high hydrothermal stability, their ability to impart shape selectivity into product distributions, and the reproducibility with which they can be synthesized and modified. Each of these advantages are directly from their crystalline structure.

Nearly 100 zeolite structure types are known, but only a handful are used commercially, due to economic and safety issues associated with syntheses of the more novel types. Some zeolites that have found application as solid acids are shown in Figure 2.5, grouped into small, medium, and large pore types. Access to the internal surfaces of small pore zeolites is controlled by openings bounded by rings containing eight tetrahedral cations and eight oxygens (eight-membered rings or 8MRs). Medium-pore zeolites, such as ZSM-5, possess pore systems bounded by 10MRs, and large-pore zeolites, such as zeolite Y, mordenite, and zeolite B have pore systems bounded by 12MRs.

Zeolites are converted to the protonic H-form (e.g., H-ZSM-5) by calcining ammonium-exchanged forms. This may result in migration of some framework aluminum into extra-framework sites and increase of the Si/Al ratio of the framework.

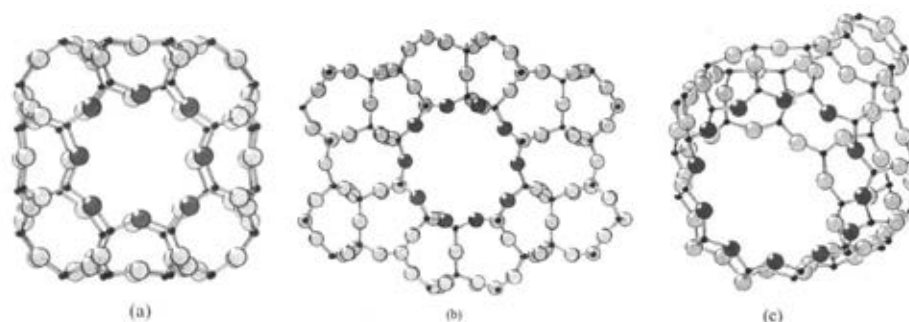


Figure 2.5 Diagrams of elements of the frameworks of (a) the small pore zeolite Rho, (b) the medium-pore zeolite ZSM-5, and (c) the large-pore zeolite Y. Tetrahedral (aluminum and silicon) cations are represented by small black spheres, and oxygens are represented by larger spheres. Oxygens of selected rings that define access to the internal pore systems are highlighted in dark gray.

This results in larger bond angles and higher acidities than those obtained in amorphous silica-alumina. Further fine-tuning of acidity and pore size is possible by cation exchange. Moreover, the active sites are spread throughout the entire internal surface so that bulk techniques can be used to study them.

2.3.1.2 Zeolite Types

There are about 40 known natural zeolites and over 150 zeolites which have been synthesized. Of this number, only a few have found commercial applications. Table 2 shows properties of the major synthetic zeolites. The zeolites with applications to FCC are Type X, Type Y, and ZSM-5. Both X and Y zeolites have essentially the same crystalline structure. The X zeolite has a lower $\text{SiO}_2/\text{Al}_2\text{O}_3$ ratio than the Y zeolite. The X zeolite also has a lower thermal and hydrothermal stability than the Y zeolite. ZSM-5 is a versatile zeolite that increases olefin yields and octane.

Table 2.2 Properties of major synthetic zeolites

Zeolite type	Pore Size Dimension (°A)	Silica to Alumina Ratio	Application
Zeolite A	4.1	2 - 5	Detergent manufacturing
Faujasite	7.4	3 – 6	Catalytic cracking and Hydrocracking
ZSM-5	5.2 x 5.8	30 – 200	Xylene isomerization, Benzene alkylation, Catalytic cracking, Catalytic dewaxing, and Methanol conversion
Mordenite	6.7 x 7.0	10 – 12	Hydro-isomerization and dewaxing

2.3.1.3 Zeolites as Supports

Zeolites make excellent candidates for catalyst supports due to their stability, high surface area, and probably most importantly, the regularity of their pore structure (van Bekkum., *et al.* 1991, Thomas and Thomas 1997). The well-defined pore sizes of zeolites mean that when used as catalysts or supports they can impose selectivity on the reaction products by restricting access of reactants to the active site and the formation of certain transition states. The cationic sites in zeolites can be substituted with metal cations, thus introducing potentially new catalytic species into the structure. In the majority of cases calcination and reduction are carried out on the metal cations to form neutral metal atoms or groups of atoms which act as the catalytically active site. Zeolites can therefore be used as supports for metal cations that are active catalysts.

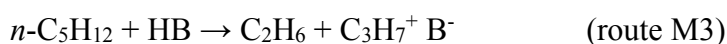
One advantage of zeolites supports is the ability to isolate metal atoms in the pores and so prevent sintering of the metal atoms, which would greatly reduce the effective surface area of the catalyst. However, to prevent agglomeration of the metal it is important to control all the stages in the preparation to avoid atom migration.

To explore the effect of pore caliber in *n*-pentane catalytic cracking reaction, Xu Hou and his co-workers were examined the conversion of *n*-pentane over HZSM-35 and H-Beta, HZSM-5 zeolite was investigated. They found that the changes in zeolite pore caliber have significantly affected the product distribution, while HZSM-5 zeolite which is the middle pore caliber zeolites presented in a highest selectivity to light olefins compared to HZSM-35 and H-Beta. Moreover, the increasing in pore caliber affected the propylene to ethylene ratio. Thus, they concluded that the appropriate zeolites for *n*-pentane catalytic cracking is HZSM-5.

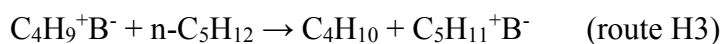
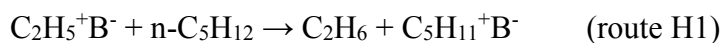
2.3.1.4 Possible Reaction Pathways for *n*-Pentane Cracking

The general reaction pathways are shown as follows:

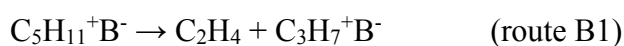
(1) Initial reactions are the monomolecular protolytic cracking of *n*-pentane generating H₂, CH₄, C₂H₆, and C₃H₈ together with carbenium ions of C₅H₁₁⁺, C₄H₉⁺, C₃H₇⁺, and C₂H₅⁺ (routes M1-M4), respectively.

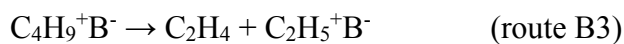


(2) Hydride transfer reaction would take place between *n*-pentane molecules and the generated carbenium ions giving pentane, butane, propane, ethane, and C₅H₁₁⁺ ions (routes H1-H4), respectively.

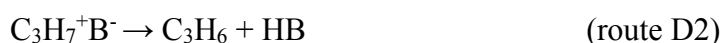


(3) At the same time, the specific carbenium ions, such as C₄H₉⁺ or C₅H₁₁⁺, may release light olefins through β-scission (routes B1-B3).





(4) At last, the deprotonation of carbenium ions gives an olefin whilst restores acid sites (routes D1-D3).



(5) In addition, side reactions such as oligomerization, isomerization, cyclization, aromatization, dehydrogenation, etc, may be also involved in the reaction system, enhancing the further conversion and complexity of products.

Table 2.3 Possible reaction pathways for *n*-pentane cracking over zeolites

Products	Pathway	Route
H ₂	$\text{C}_5 \rightarrow \text{C}_5^+ + \text{H}_2$	M1
C ₂ H ₄	$\text{C}_2^+ \rightarrow \text{C}_2^=$ $\text{C}_5^+ \rightarrow \text{C}_2^= + \text{C}_3^+$ $\text{C}_4^+ \rightarrow \text{C}_2^= + \text{C}_2^+$	D1 B1 B3
C ₃ H ₆	$\text{C}_3^+ \rightarrow \text{C}_3^=$ $\text{C}_5^+ \rightarrow \text{C}_3^= + \text{C}_2^+$	D2 B2
C ₄ H ₈	$\text{C}_4^+ \rightarrow \text{C}_4^=$	D3
CH ₄	$\text{C}_5 \rightarrow \text{C}_4^+ + \text{C}_1$	M2
C ₂ H ₆	$\text{C}_5 \rightarrow \text{C}_3^+ + \text{C}_2$ $\text{C}_2^+ + \text{C}_5 \rightarrow \text{C}_5^+ + \text{C}_2$	M3 H1
C ₃ H ₈	$\text{C}_5 \rightarrow \text{C}_2^+ + \text{C}_3$ $\text{C}_3^+ + \text{C}_5 \rightarrow \text{C}_5^+ + \text{C}_3$	M4 H2
C ₄ H ₁₀	$\text{C}_4^+ + \text{C}_5 \rightarrow \text{C}_5^+ + \text{C}_4$	H3

2.3.1.5 Deactivation of Catalyst

Catalyst deactivation mainly happens from the coke decomposition. The coke formation over HZSM-5 zeolite catalyst in these reactions would decrease the efficiency conversion of reaction by removal of acid sites. For these reasons, it is very interesting to find the way that can control the coke formation also maintain activity and stability of catalyst.

2.4 Modification of Zeolite

2.4.1 Metal Incorporation

Metal-incorporation is an effective method to improve the light olefins production in naphtha cracking over zeolites.

Very recently, Xu Hou and his co-workers studied the modification of zeolite which could enhance light olefins production through *n*-pentane catalytic cracking over HZSM-5 based catalysts. The modified catalysts which are Zr/HZSM-5 and Ag/HZSM-5 were obtained by impregnation method. It was found that the modified catalysts and regenerated catalyst achieved a higher light olefins yield compared to HZSM-5 catalyst.

At 550 °C, the Zr/HZSM-5 catalyst exhibited a lower light olefins selectivity but higher ethylene and propylene yield also higher conversion when compared to HZSM-5 and Ag/HZSM-5 catalysts. The authors concluded that Zr metal had the ability to enhance the interaction between the reactant molecules and brønsted acid site or carbenium ions, resulted in the promotion of protolytic cracking of *n*-pentane. For Ag/HZSM-5, it is exhibited in the promotion of light olefins selectivity, propylene and ethylene yield at the reaction temperature of 400, 450 and 500 °C when compared to HZSM-5 and Zr/HZSM-5 catalyst, while dramatically decreased when the reaction temperature raised up to 550 °C which probably from the coke formation. They interpreted that Ag metal can promote the light olefins formation from the dehydrogenation cracking over Ag sites.

Therefore, this could be summarized that Zr/HZSM-5 gives a good conversion and stability at high reaction temperature but still not enough for reaching the desirable performance of light olefins production. The addition of second metal

which has the ability in dehydrogenation reaction to Zr/HZSM-5 catalysts would become more challenge in enhancing the light olefins production and control the ratio of propylene to ethylene.

Silver (Ag) metal which is a noble metal that provided an active activity is considered as one of the interesting metals for the promotion of dehydrogenation reaction in *n*-pentane catalytic cracking.

Ono and Baba (2015) reported that Ag species from Ag/HZSM-5 catalyst significantly enhance the dehydrogenation of the alkanes due to the heterolytic dissociation of the alkanes into carbenium ions and hydride species, while it represses the C–C bond cleavage. They studied the catalyst activity of Ag/HZSM-5 on the light alkanes aromatization, it was found that Ag/HZSM-5 provided a high conversion and acts as a dehydrogenation catalyst for converting alkanes into alkenes.

Other interesting noble metals is Palladium (Pd). The study of the effect of noble metal catalysts on perhydro-N-ethylcarbazole catalytic dehydrogenation was investigated.(Yang *et al.*, 2014). Those noble metals including Ru, Rh, Pd and Pt on alumina support were used for this study. It was found that supported Pd catalyst achieved the highest initial catalytic activity for the dehydrogenation process and followed by Pt, Ru and Rh catalysts, respectively. Moreover, only supported Pt and Pd catalysts can accomplished fully dehydrogenation.

The ethane dehydrogenation over Pd-In intermetallic alloy nanoparticles catalysts was examined by Wu *et al.* (2016). The ethane dehydrogenation reaction was taken place at 600 °C. They were found that monometallic Pd catalysts on silica supported can reached the dehydrogenation selectivity 53% at 15% conversion. Besides, the addition of In into Pd increased the dehydrogenation selectivity close to 100%. They concluded that addition of In atom was isolated the Pd sites, resulted in the olefin and dehydrogenation reaction selectivity increases.

Another interesting candidate is Nickel (Ni) metal which is a transition metal that has a lower price when compared to the Ag and Pd metal. Furthermore, it can provide a high activity especially for dehydrogenation reactions.(Resasco *et al.*, 1994)

The study of *i*-butane and *n*-butane cracking on Ni/HZSM-5 (SiO₂/Al₂O₃ ratio of 25) at the temperature of 500 °C was investigated by Maia *et al.* (2011). They found that the effect of Ni addition on the support in order to promote the initially dehydrogenation from *i*-butane to *i*-butene before further cracking over Bronsted acid site that provided by HZSM-5. The results showed that the addition of Ni significantly promote the dehydrogenation reaction when compared to the obtained *i*-butane from pure HZSM-5 and Ni/HZSM5 which can be observed from the *i*-butene selectivity that increased from 13% to 20%.



242044977

CU IThesis 6171002063 thesis / recv: 31072563 03:53:59 / seq: 17

CHAPTER 3

EXPERIMENTAL

Materials and Equipment

Materials:

Feedstock

n-Pentane (C₅H₁₂, 99% purity) was supplied from RCI Labscan, Thailand.

Gases

1. The high purity (HP) hydrogen (99.99% purity) was used for FID detector that supplied from Praxair, Thailand.
2. The high purity (HP) nitrogen (99.99% purity) was used for purging catalysts after reaction testing and carrier gas that supplied from Air Liquide, Thailand.
3. The zero-grade air (99.99% purity) was used for FID detector that supplied from S. I. Technology, Thailand.
4. The ultra-high purity (UHP) helium (99.99% purity) was used for TCD detector that supplied from Praxair, Thailand.
5. The 5 vol% oxygen balanced in helium was used for the temperature-programmed oxidation (TPO) measurement and oxidation treatment that supplied from Praxair, Thailand.
6. The 5 vol% hydrogen balanced in argon was used for the temperature-programmed reduction (TPR) measurement that supplied from Praxair, Thailand.

Chemicals

1. Zirconium (IV) oxide chloride (ZrOCl₂, 98% purity) was obtained from PTT Global Chemical Public Company Limited (GC), Thailand.
2. Silver nitrate (AgNO₃, ≥ 99.0% purity) was supplied from Sigma Aldrich, USA.
3. Palladium (II) chloride (PdCl₂, 99% purity) was supplied from Sigma Aldrich, USA.
4. Nickel (II) nitrate hexahydrate (Ni(NO₃)₂·6H₂O, 97% purity) was supplied from Sigma Aldrich, USA.
5. The commercial ZSM-5 zeolite (SiO₂/Al₂O₃ ratio 23, 50 and 80) was supplied from Zeolyst, USA.

Equipment:

1. Catalytic testing system consisting of gas cylinders, mass flow controller (Aalborg-AGFC171S), furnace, and 1/2" O.D. x 19.5" long Pyrex reactor.
2. Rigaku X-ray diffractometer.
3. X-Ray fluorescence spectrometer (WDXRF) – XRF (WDXRF)
4. BELCAT II analyzer for temperature programmed reduction, temperature programmed oxidation and temperature programmed desorption (TPDRO)
5. Transmission electron microscope – TEM (1400)
6. Hamilton syringe pump.
7. Leco CHNS elemental analyzer
8. Shimadzu GC-17A gas chromatograph equipped with a capillary HP- PLOT/Al₂O₃ "S" deactivated column.

Experimental Procedures**3.1 Catalyst Preparation****3.1.1 Incipient Wetness Impregnation**

ZrOCl₂, AgNO₃, PdCl₂ and Ni(NO₃)₂·6H₂O were dissolved in deionized (DI) water to form the aqueous solution of the metal precursors. Then the metal-containing solution was added to a catalyst support that already calcined (HZSM-5 with SiO₂/Al₂O₃ ratio 23) by incipient wetness impregnation. The catalyst was then dried at room temperature. It was equivalent to 3 wt% of metal per gram zeolite for monometallic and 1.5 wt% of each metal component for bimetallic catalysts. After excess water was evaporated, the impregnated samples were dried at 120 °C overnight and then calcined with air at 550 °C for 5 h. The modified catalysts were denoted as 3Zr/HZSM-5, 1.5Ag1.5Zr/HZSM-5, 1.5Pd1.5Zr/HZSM-5 and 1.5Ni1.5Zr/HZSM-5.

For the 1.5Ag1.5Zr/ZSM-5 catalysts with different SiO₂/Al₂O₃ ratios, The catalysts were prepared by the same method as mentioned above but using HZSM-5 with SiO₂/Al₂O₃ ratio of 23, 50 and 80. Then, those catalysts were denoted as 1.5Ag1.5Zr/HZSM-5(23), 1.5Ag1.5Zr/HZSM-5(50) and 1.5Ag1.5Zr/HZSM-5(80), respectively.

3.1.2 Catalytic Activity Testing

The *n*-pentane cracking test was carried out in a continuous flow fixed-bed reactor. In each test, 0.2 g of fresh catalyst was packed in a 1/2" Pyrex reactor, the modified catalyst was reduced by hydrogen with flow rate of 30 mL/min at 550 °C for 2 h. Then, *n*-pentane feed was continuously injected by a syringe pump and preheated to 70 °C with a flow rate of 0.027 ml/min for obtaining WHSV of 5 h⁻¹. Nitrogen is used as a carried gas with flow rate of 30 mL/min. The reaction was performed at 550 °C under atmospheric pressure. The products were analyzed by a gas chromatograph using a Shimadzu 17A-GC equipped with an HP-PLOT/Al₂O₃ "S" deactivated capillary column. The GC column temperature was programmed to obtain an adequate separation of the products. The temperature was first kept constant at 40 °C for 3 min, then linearly ramped up to 70 °C with ramp rate 15 °C/min, ramped up to 170 °C with ramp rate 5 °C/min and ramped up to 195 °C with ramp rate 1 °C/min, respectively.

The conversion of feed and selectivity is defined as follows;

$$n\text{-pentane conversion (\%)} = \frac{\text{wt. of feed converted} \times 100\%}{\text{wt. of } n\text{-pentane}}$$

$$\text{Selectivity to product } i \text{ (\%)} = \frac{\text{wt. of product } i \times 100\%}{\text{Total wt. of products}}$$

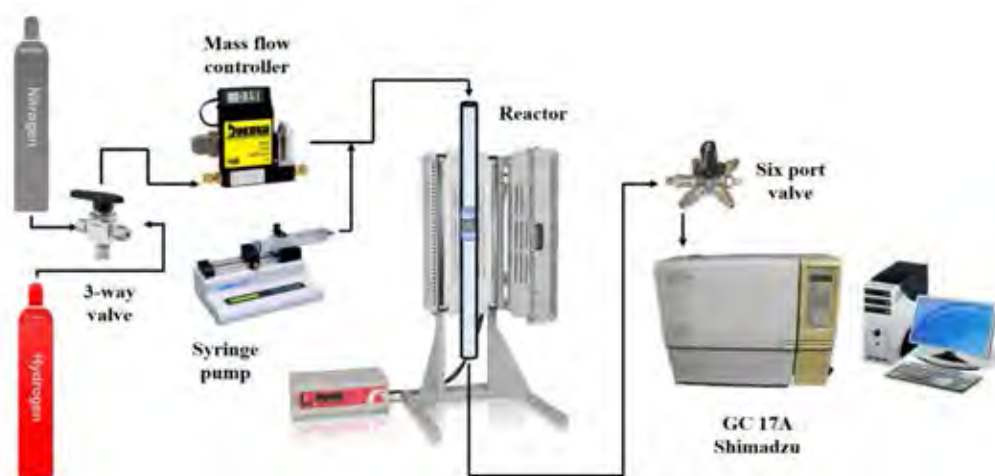


Figure 3.1 Schematic of the experimental set-up for *n*-pentane cracking.

3.1.3 Catalyst Characterization

3.1.3.1 Temperature Programmed Reduction of Hydrogen (H_2 -TPR)

H_2 -TPR is a useful technique for the characterization of metal oxide catalysts. The resulting TPR profile contains qualitative information on the oxidation state of the reducible species present. Temperature programmed reduction (TPR) was performed on the fresh calcined catalysts. For each run, 0.05 g of sample was packed in a 0.25 " O.D quartz tube reactor. TPR runs were conducted using a heating rate of 10 °C/min in a flow of 5% H_2 /Ar (30 mL/min) up to 800 °C.

3.1.3.2 Temperature Programmed Oxidation (TPO)

TPO is used for the determination of the amount and the chemical state of carbon on deactivated catalysts during the reaction. TPO of the spent catalysts was performed in a continuous flow of 2% O_2 in He while the temperature was linearly increased to 900 °C with a heating rate of 10 °C/min. The oxidation was conducted in a 1/4" quartz tube fixed-bed reactor. Prior to the test, the spent catalyst was dried at 110 °C overnight, weighted (10 mg), and placed between two layers of quartz wool inside the quartz tube. The sample was further purged at room temperature by flowing 2% O_2 in He for 30 min before the TPO is started. The CO_2 produced by the oxidation of the coke species was converted to methane in a separate methanizer filled with 15% Ni/ Al_2O_3 and operated at 415 °C. The evolution of methane was analyzed using an FID detector.

3.1.3.3 Temperature Programmed Desorption (TPD) of Ammonia

TPD of ammonia is a widely used method for the characterization of acidity in catalysts due to the simplicity of the technique. First, 0.05 g of sample was pretreated at 300 °C in a flow of N_2 for 30 min and 10% NH_3 in He for 30 min. After the pretreatment, purging line with N_2 , then, flowing with He and heated up to 900 °C with ramp rate of 10 °C/min and hold for 30 min.

3.1.3.4 X-ray Fluorescence Spectroscopy (XRF)

The quantitative and qualitative elemental analysis of the ZSM-5 zeolite and modified ZSM-5 were analyzed by XRF technique. With a primary X-ray excitation source from an X-ray tube, the X-ray can be absorbed by the atom, and transfer all its energy to an innermost electron. During the process, if the primary X-



ray has sufficient energy, electrons are ejected from the inner shell, creating vacancies. These vacancies present an unstable condition for the atom. As the atom returns to its stable condition, electrons from the outer shells are transferred to the inner shells, and the process gives off a characteristic X-ray, whose energy is the difference between the two binding energies of the corresponding shells. Because each element has a unique set of energy levels, each element produces X-rays at a unique set of energies, allowing one to non-destructively measure the elemental composition of a sample. The intensities of observed lines for a given atom vary according to the amount of that atom present in the specimen.

3.1.3.5 *N₂ Adsorption/Desorption Measurement*

Surface area, total pore volume, micropore volume, and mesopore volume of the samples were determined by using BET method on a Quantachrom/Autosorb 1-MP instrument. Firstly, the sample was outgassed to remove the humidity and volatile adsorbents adsorbed on surface under vacuum at 300 °C for 12 h prior to the analysis. Next, N₂ was purged to adsorb on surface. The quantity of gas adsorbed onto or desorbed from their solid surface at some equilibrium vapor pressure by static volumetric method will be measured. The solid sample was maintained at a constant temperature of the sample cell until the equilibrium is established. This volume-pressure data was used to calculate the BET surface area.

3.1.3.6 *X-ray Diffraction (XRD)*

XRD is a technique that provides detailed information of the crystallographic structure, chemical composition, and physical properties of materials. The relative crystallinities of the ZSM-5 zeolite and modified ZSM-5 were analyzed by a Rigaku X-ray diffractometer with Cu tube for generating CuK α radiation ($\lambda=1.5418 \text{ \AA}$) at room temperature. When an X-ray beam hits a sample and is diffracted, we can measure the distances between the planes of the atoms that constitute the sample by applying Bragg's Law. Bragg's Law is: $n\lambda = 2d \sin\theta$, where the integer n is the order of the diffracted beam, λ is the wavelength of the incident X-ray beam, d is the distance between adjacent planes of atoms (the d -spacings), and θ is the angle of incident of the X-ray beam. The characteristic set of d -spacings generated in a typical X-ray scan provides a unique "fingerprint" of the mineral or minerals present in the sample.

3.1.3.7 Leco CHNS Elemental Analyzer

The CHN628 series elemental determinator is used to determine nitrogen, carbon/nitrogen, and carbon/hydrogen/nitrogen in organic matrices. The instrument utilizes a combustion technique and provides a result within 4.5 minutes for all the elements being determined. The instrument features custom software operated through an external PC to control the system operation and data management. The final results are typically displayed in weight percent or parts-per-million but can be displayed in other custom units or conversions such as percent total protein, moisture corrected, and others.

3.1.3.8 Transmission Electron Microscope (TEM)

TEM is one of the common methods used to analyze the quality, shape, size and density of quantum wells, wires and dots. The TEM operates on the same basic principles as the light microscope but uses electrons instead of light. Because the wavelength of electrons is much smaller than that of light, the optimal resolution attainable for TEM images is many orders of magnitude better than that from a light microscope. Thus, TEMs can reveal the finest details of internal structure in some cases as small as individual atoms. The samples were prepared by the Ultramicrotome Leica EM UC7 that provides easy preparation of semi- and ultrathin sections as well as perfect, smooth surfaces samples. The TEM images of the catalysts were acquired in JEM-1400 Flash Electron Microscope.



242044977

CHAPTER 4

RESULTS AND DISCUSSION

4.1 Catalyst Characterization

4.1.1 X-ray Diffraction

The XRD patterns of HZSM-5, modified HZSM-5 with SiO₂/Al₂O₃ ratio of 23 catalysts and 1.5Ag1.5Zr/HZSM-5 catalysts with different SiO₂/Al₂O₃ ratios of 23, 50 and 80 are given in Figures 4.1 and 4.2. Characteristic diffraction peaks at $2\theta = 7-9, 22-25^\circ$ are considered as the fingerprints of MFI structure that corresponded to (1 0 1), (2 0 0), (5 0 1), (1 5 1) and (3 0 3) crystal faces, respectively (Diao *et al.*, 2015). As shown in Figure 4.1, all of the modified HZSM-5 catalysts exhibited characteristic diffraction peaks similar to HZSM-5. However, the diffraction peaks of metal oxide were not detected. This could indicate the well dispersion of metal oxide on the zeolite. (Jodaei *et al.*, 2011).

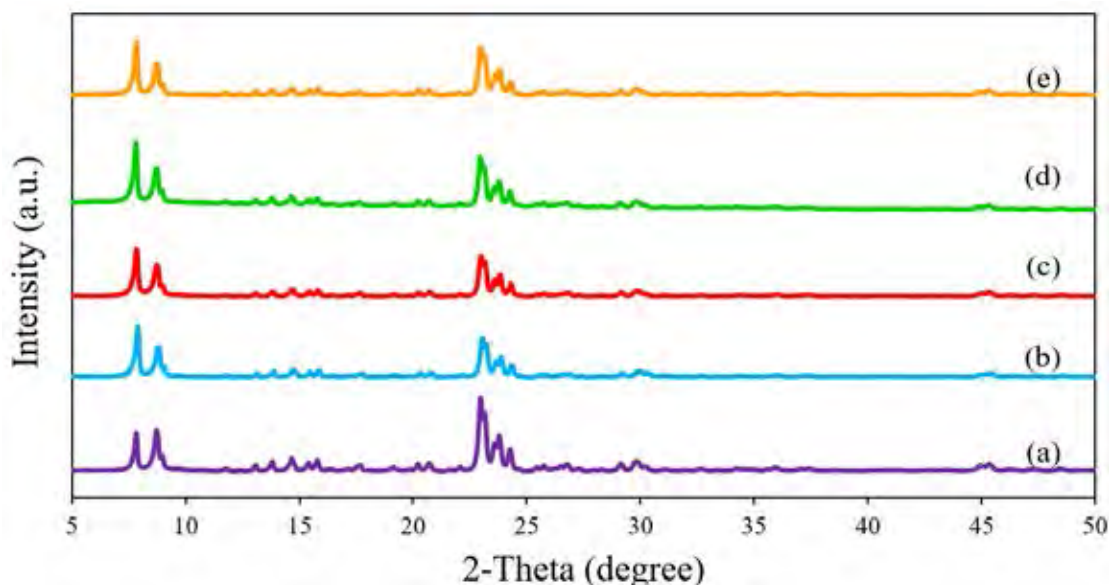


Figure 4.1 XRD patterns of (a) HZSM-5, (b) 3Zr/HZSM-5, (c) 1.5Ag1.5Zr/HZSM-5, (d) 1.5Pd1.5Zr/HZSM-5 and (e) 1.5Ni1.5Zr/HZSM-5 with SiO₂/Al₂O₃ ratio 23.

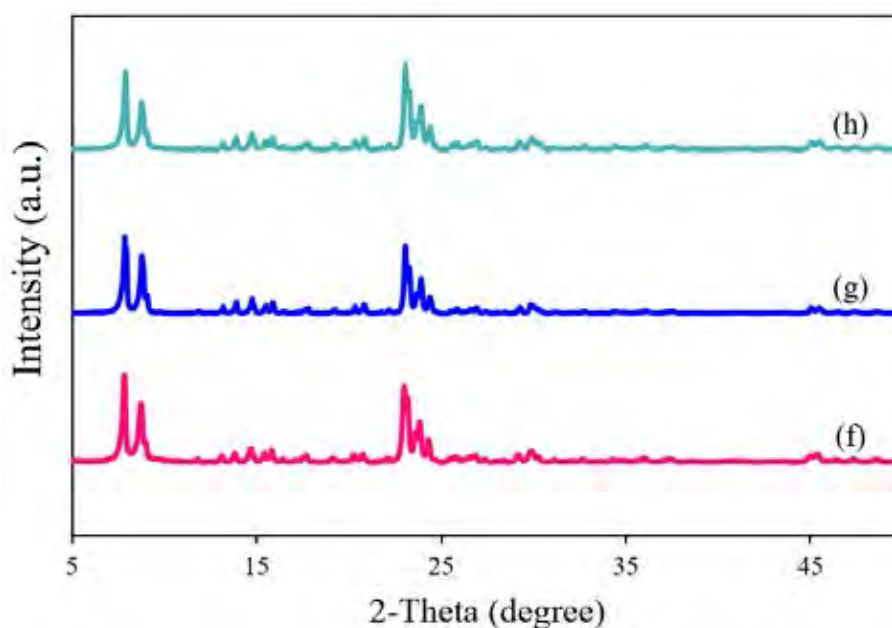


Figure 4.2 XRD patterns of (f) 1.5Ag1.5Zr/HZSM-5 (23), (g) 1.5Ag1.5Zr/HZSM-5 (50) and (h) 1.5Ag1.5Zr/HZSM-5 (80).

4.1.2 Brunauer–Emmett–Teller (BET) Surface Analyzer and X-ray Fluorescence Spectrometer (XRF)

The textural properties of HZSM-5 and modified HZSM-5 catalysts are summarized in Table 4.1. From the results of parent HZSM-5 and modified HZSM-5 with $\text{SiO}_2/\text{Al}_2\text{O}_3$ ratios of 23, 50 and 80, it was found that the surface area and pore volume decreased after the metal addition, especially for bimetallic nickel and zirconium catalyst. This could be due to the blockage from metal oxide species presence on the catalyst supports.

The actual metal composition of modified catalysts with $\text{SiO}_2/\text{Al}_2\text{O}_3$ ratio of 23 analysed by XRF are given in Table 4.1.

Table 4.1 The textural properties and element composition of catalysts

Catalyst	Surface area ^a (m ² /g)	Pore volume ^b (mL/g)	Metal composition (%wt.)			
			Zr	Pd	Ni	Ag
HZSM-5 (23)	329	0.236	-	-	-	-
HZSM-5 (50)	308	0.275	-	-	-	-
HZSM-5 (80)	355	0.193	-	-	-	-
3Zr/HZSM-5 (23)	294	0.110	3.44	-	-	-
1.5Pd1.5Zr/HZSM-5 (23)	299	0.136	1.86	1.09	-	-
1.5Ni1.5Zr/HZSM-5 (23)	237	0.100	1.31	-	0.96	-
1.5Ag1.5Zr/HZSM-5 (23)	260	0.135	1.26	-	-	0.93
1.5Ag1.5Zr/HZSM-5 (50)	304	0.207	N/A			
1.5Ag1.5Zr/HZSM-5 (80)	345	0.151				

^a Estimated by the BET method

^b Estimated by the t-plot method

4.1.3 Transmission Electron Microscope (TEM)

The dispersion of metal oxide over HZSM-5 support was observed by transmission electron microscope as shown in Figure 4.3. In Figure 4.3 (a), the calcined parent HZSM-5 zeolite obviously showed the crystals presenting hexagonal plate shape (Silva *et al.*, 2019). In Figure 4.3 (b), TEM image of 3Zr/HZSM-5 presents the high dispersion of ZrO₂ on HZSM-5 support. However, some of larger ZrO₂ particles exhibited on the HZSM-5 support, indicating that the agglomeration of ZrO₂ was occurred.

In Figure 4.3 (c), TEM image of 1.5Pd1.5Zr/HZSM-5 obviously shows the high dispersion of metal oxide particles on the support. However, it cannot define the certainly location of PdO and ZrO₂ on HZSM-5 zeolite due to the similar particle size between PdO and ZrO₂. In Figure 4.3 (d), TEM image of 1.5Ni1.5Zr/HZSM-5 showed that NiO particles were highly dispersed throughout the support, while the ZrO₂ cannot clearly distinguished between ZrO₂ and small NiO particles. In Figure 4.3 (e), TEM image of 1.5Ag1.5Zr/HZSM-5 showed the high dispersion of Ag₂O and ZrO₂ particles on the support and also exhibited the agglomeration of Ag₂O particles on the support. However, Ag₂O and ZrO₂ particles could not be distinguished due to their small similar particle size as presented in Figure 4.3 (f).

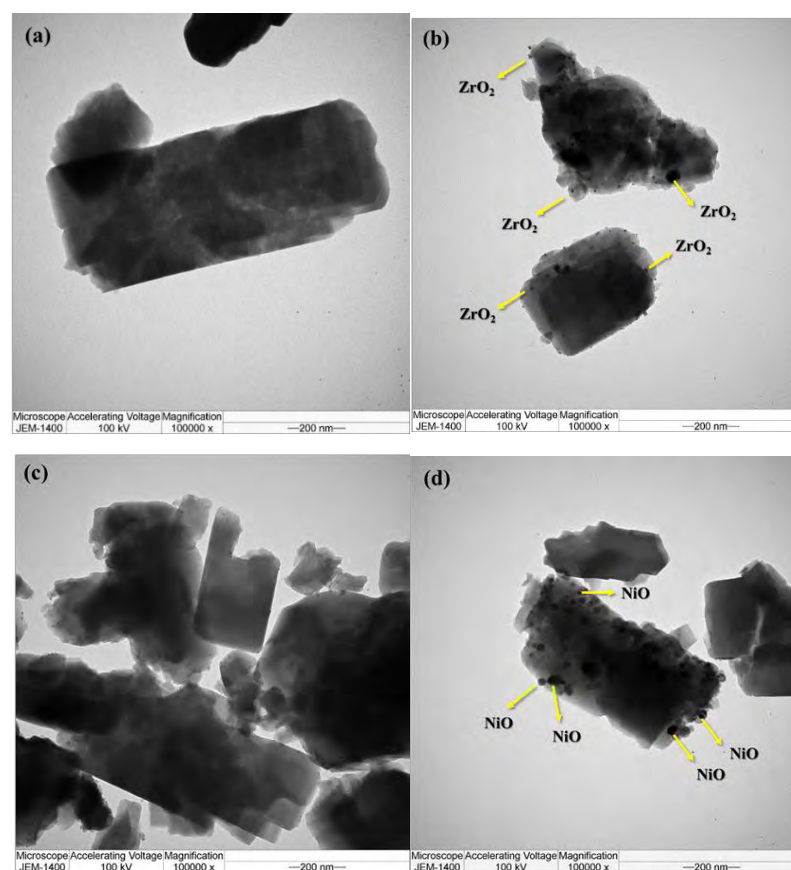


Figure 4.3 TEM images of calcined (a) parent HZSM-5, (b) 3wt%Zr/HZSM-5, (c) 1.5wt%Pd1.5wt%Zr/HZSM-5, (d) 1.5wt%Ni1.5wt%Zr/HZSM-5, (e) 1.5wt%Ag1.5wt%Zr/HZSM-5 (1) and (f) 1.5wt%Ag1.5wt%Zr/HZSM-5 (2) catalysts.

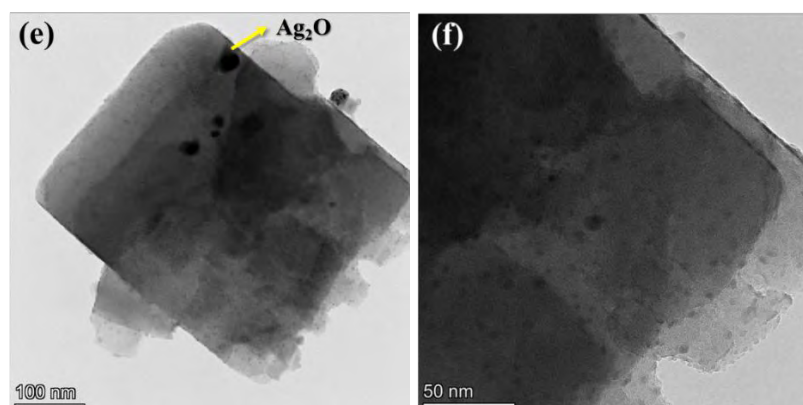


Figure 4.3 (Cont.) TEM images of calcined (a) parent HZSM-5, (b) 3wt%Zr/HZSM-5, (c) 1.5wt%Pd1.5wt%Zr/HZSM-5, (d) 1.5wt%Ni1.5wt%Zr/HZSM-5, (e) 1.5wt%Ag1.5wt%Zr/HZSM-5 (1) and (f) 1.5wt%Ag1.5wt%Zr/HZSM-5 (2) catalysts.

4.1.4 Temperature Programmed Desorption of Ammonia (NH₃-TPD)

The NH₃-TPD was applied to analyze the total amount of surface acid site or the acid density of the catalysts. The NH₃-TPD results from HZSM-5 and modified HZSM-5 catalysts with different SiO₂/Al₂O₃ ratios are shown in Figure 4.4 and Table 4.2. All of the NH₃-TPD results can be divided into two types of desorption peaks as listed in Table 4.2. The quantities of weak and strong acid sites were measured by the amount of ammonia desorption at 100-300 °C and 350-550 °C, respectively. The presence of zirconium oxide, palladium oxide and nickel oxide resulted in the increase of total acid site, especially strong acid site when compared to the HZSM-5 catalyst. For the Zr modification on HZSM-5 catalyst, the presence of zirconium oxide enhanced the strong acid site. This could indicate that the introduction of Zr oxide species in the zeolite matrix created other types of surface acidity with lower binding strength than the pure zeolite material. (Wang *et al.*, 2019).

When Pd was presented on the Zr-based HZSM-5 catalyst, the NH₃ desorption peak at around 220 °C was slightly decreased, while the broad NH₃ desorption peak at around 420 °C was increased. (Lee *et al.*, 2018).

In case of the Ni addition on Zr/HZSM-5, the Ni modification on Zr/HZSM-5 provided the same results as 1.5Pd1.5Zr/HZSM-5 catalysts, while the strong NH₃ desorption peak was insignificantly increased. This could be explained

from the strong desorption of NH_3 on the acidic Al-OH and Al-OH-Si in the surface and structure. (Weng *et al.*, 2015).

On the other hand, the result from bimetallic silver and zirconium exhibited in an opposite way. The amount of total acid site when compared to other catalysts was clearly observed. This could possibly due to the blockage of Ag species on the acid site of Zr/ZSM-5 catalysts, resulting in decrease the amount of weak acid site, strong acid site and total acid site as compared to other catalysts.

In comparison between the total acidity of 1.5Ag1.5Zr/HZSM-5 with different $\text{SiO}_2/\text{Al}_2\text{O}_3$ ratios of 23, 50 and 80, the decrease in $\text{SiO}_2/\text{Al}_2\text{O}_3$ ratio increased the total amount of acid site including weak and strong acid sites. This could be due to the increase in extra-framework aluminum content. (Shirazi *et al.*, 2008).

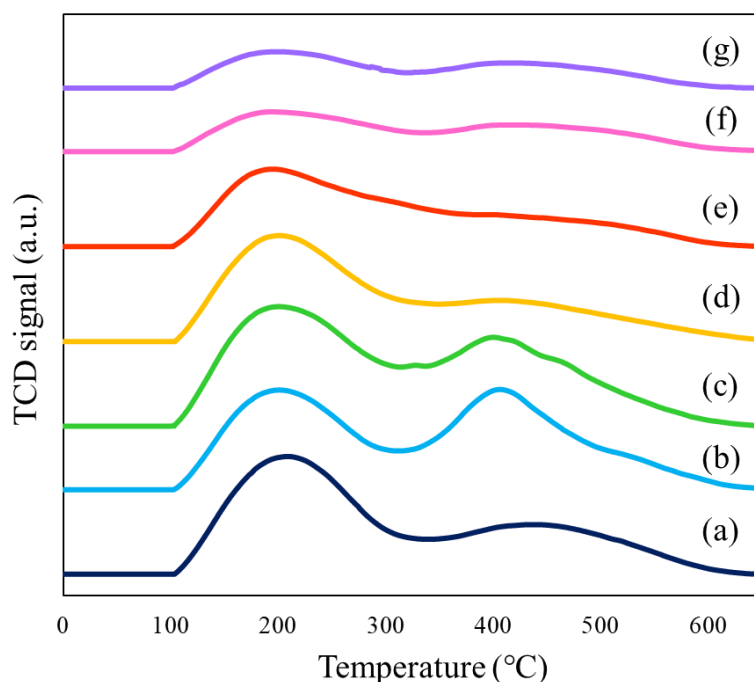


Figure 4.4 NH_3 -TPD profiles of (a) HZSM-5 (23), (b) 3Zr/HZSM-5 (23), (c) 1.5Pd1.5Zr/HZSM-5 (23), (d) 1.5Ni1.5Zr/HZSM-5 (23), (e) 1.5Ag1.5Zr/HZSM-5 (23), (f) 1.5Ag1.5Zr/HZSM-5 (50) and (g) 1.5Ag1.5Zr/HZSM-5 (80).

Table 4.2 The total acid amount of HZSM-5 and modified HZSM-5 catalysts, detected by NH₃-TPD

Catalyst	Acid amount (mmol/g)		
	Weak acid	Strong acid	Total acid
HZSM-5 (23)	0.733	0.553	1.286
3Zr/HZSM-5 (23)	0.603	0.838	1.441
1.5Pd1.5Zr/HZSM-5 (23)	0.698	0.850	1.548
1.5Ni1.5Zr/HZSM-5 (23)	0.675	0.700	1.375
1.5Ag1.5Zr/HZSM-5 (23)	0.371	0.529	0.900
1.5Ag1.5Zr/HZSM-5 (50)	0.285	0.359	0.644
1.5Ag1.5Zr/HZSM-5 (80)	0.239	0.286	0.525

4.1.5 Temperature Programmed Reduction of Hydrogen (H₂-TPR)

Temperature programmed reduction is used to evaluate the reduction temperature of modification catalysts. The reducibility of metal oxide is depending on their location on the support and their interaction between metal and support. The H₂-TPR profiles of HZSM-5 and modifies HZSM-5 catalysts were recorded in the range of 30–750 °C as shown in Figure 4.5. Figure 4.5 (b) shows the reducibility of ZrO₂ particles on HZSM-5, it was no hydrogen consumption peaks, resulting in the low reducibility of ZrO₂ particles (Hou *et al.*, 2019). The result from 1.5Pd1.5Zr/HZSM-5 catalyst is shown in Figure 4.5 (c), the negative hydrogen consumption peak at the temperature around 50-80 °C was observed. This could possibly due to the desorption of weakly adsorbed hydrogen and the decomposition of PdH_x (He *et al.*, 2010). This result suggested that PdO in H₂ atmosphere was easily reduced to the metallic Pd even at the ambient temperature. The result from 1.5Ni1.5Zr/HZSM-5 catalyst is shown in Figure 4.5 (d), the hydrogen consumption peak was observed as overlapping peaks at the temperature around 400-600 °C. All nickel was reduced from Ni²⁺ to Ni⁰. (Maia *et al.*, 2010). This indicated that the obtained bimetallic Ni and Zr catalyst presence of different reducible nickel containing phases. The peaks between 400-450 °C were

assigned to the reduction of bulk NiO having weak or no interaction with the zeolite support (Popova *et al.*, 2018). For the broaden peaks above 450 °C belongs to the reduction of Ni²⁺ species that strongly interacted with support. The results from 1.5Ag1.5Zr/HZSM-5 catalyst with SiO₂/Al₂O₃ ratios of 23, 50 and 80 are shown in Figure 4.5 (e), (f) and (g). The overlapping hydrogen consumption peaks were observed at 280-400 °C which indicated the existence of more than one kind of silver species (Hou *et al.*, 2017). All silver cation in bimetallic Ag and Zr on HZSM-5 catalyst were reduced to silver metal at around 360 °C. These findings described that the Ag⁺ cations are readily reduced to metal (Kubo *et al.*, 2015).

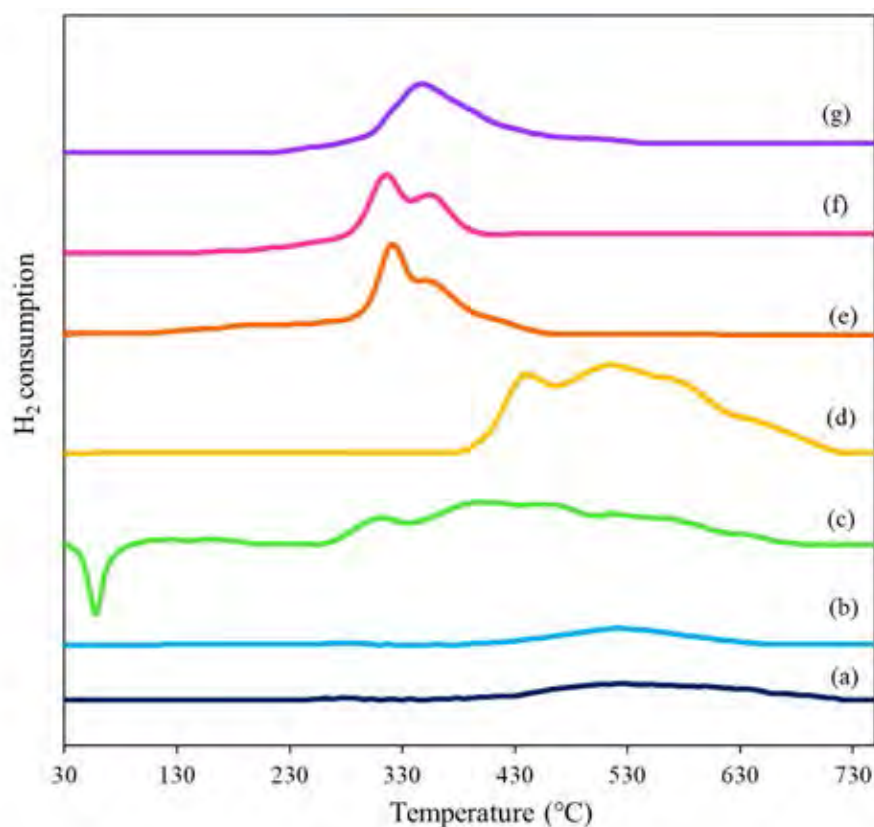


Figure 4.5 H₂-TPR profiles of (a) HZSM-5 (23), (b) 3Zr/HZSM-5 (23), (c) 1.5Pd1.5Zr/HZSM-5 (23), (d) 1.5Ni1.5Zr/HZSM-5 (23), (e) 1.5Ag1.5Zr/HZSM-5 (23), (f) 1.5Ag1.5Zr/HZSM-5 (50) and (g) 1.5Ag1.5Zr/HZSM-5 (80).

4.1.6 Temperature Programmed Oxidation (TPO) and CHNS/O Analyzer

Figure 4.6 and Table 4.3 illustrate the amount of coke deposit on the spent catalysts that analyzed by TPO technique and CHNS elemental analyzer,

respectively. The results exhibit that 1.5Ni1.5Zr/HZSM-5 catalyst provides the highest coke formation which is 26.01%wt. and observes at the temperature above 500 °C that considered as a hard coke, while 3Zr/HZSM-5 catalyst produces the lowest coke formation which is 2.92%wt when compared to other modified HZSM-5 catalysts with SiO₂/Al₂O₃ ratio of 23.

Considering the coke deposition of 1.5Ag1.5Zr/HZSM-5 catalysts with different SiO₂/Al₂O₃ ratios of 23, 50 and 80, it was found that the increase in SiO₂/Al₂O₃ ratio resulted in decreased of coke formation. This can be concluded that the decrease of catalyst acidity with increasing in SiO₂/Al₂O₃ ratio is significantly decreased the coke deposition.

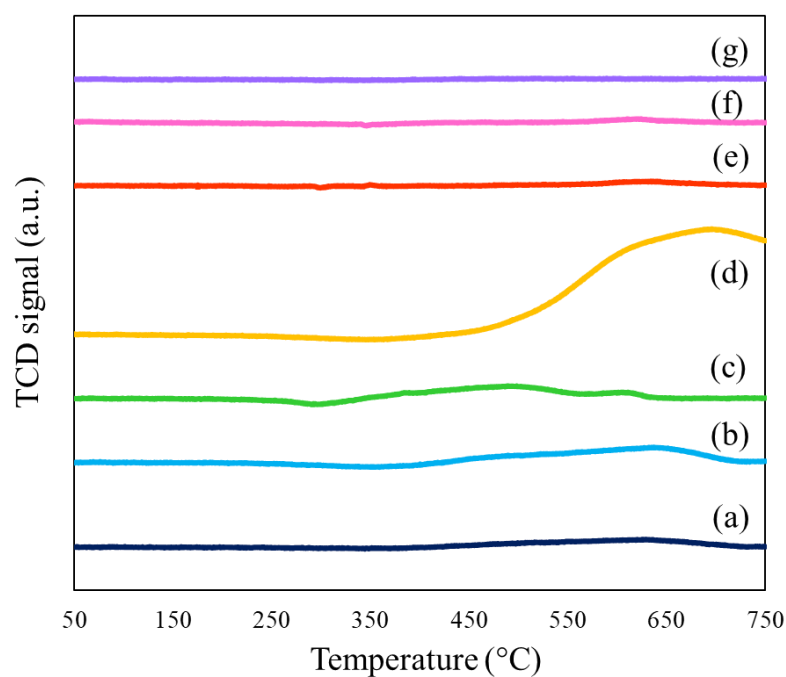


Figure 4.6 TPO profiles of (a) HZSM-5 (23), (b) 3Zr/HZSM-5 (23), (c) 1.5Pd1.5Zr/HZSM-5 (23), (d) 1.5Ni1.5Zr/HZSM-5 (23), (e) 1.5Ag1.5Zr/HZSM-5 (23), (f) 1.5Ag1.5Zr/HZSM-5 (50) and (g) 1.5Ag1.5Zr/HZSM-5 (80).

Table 4.3 Amount of carbon deposits on HZSM-5 and modified HZSM-5 catalysts after reaction

Spent catalyst	Coke (%wt.)
HZSM-5 (23)	6.07
3Zr/HZSM-5 (23)	2.92
1.5Pd1.5Zr/HZSM-5 (23)	5.91
1.5Ni1.5Zr/HZSM-5 (23)	26.01
1.5Ag1.5Zr/HZSM-5 (23)	2.05
1.5Ag1.5Zr/HZSM-5 (50)	0.73
1.5Ag1.5Zr/HZSM-5 (80)	0.44

4.2 Catalytic Activity Testing

In this part, the *n*-pentane conversion, light olefins yield and selectivity of ethylene and propylene over HZSM-5 and modified HZSM-5 catalysts were investigated. The reaction was performed at 550 °C under atmospheric pressure with *n*-pentane WHSV of 5 h⁻¹. All of the results are considered at time on stream (TOS) 3 h.

4.2.1 Effect of Second Metals Loading

At TOS 3 h, the addition of second metals on Zr/HZSM-5 catalysts affected in the product distribution and light olefins yield as shown in Figure 4.7 and 4.8, respectively. The obtained conversion from HZSM-5 and modified HZSM-5 catalysts are in ranging from 94.8% to 99.9%.

In comparison between HZSM-5 and Zr/HZSM-5 catalyst, the presence of Zr species did not significantly improve the light olefins selectivity. However, the presence of Zr species enhanced propylene selectivity and diminished in undesired products which are C₅⁺ hydrocarbons. The addition of Pd species on the Zr/HZSM-5 catalyst provided a higher propylene selectivity when compared to 3Zr/HZSM-5 catalyst. This could be possibly due to the dehydrogenation activity from Pd species.

For 1.5Ni1.5Zr/HZSM-5 catalyst, the presence of Ni species on the Zr/HZSM-5 catalyst showed the different results which is produced the lowest light olefins selectivity and highest C_5^+ products selectivity when compared to other bimetallic catalysts corresponding to the results of light olefins and light paraffins yield from 1.5Ni1.5Zr/HZSM-5 catalyst that presented in Figure 4.8. This could be attributed that Ni metal species had poor dehydrogenation activity that was observed from the lowest light olefins production. In addition, 1.5Ni1.5Zr/HZSM-5 catalyst had the lowest surface area and pore volume as shown in Table 4.1 which could be due to the agglomeration of Ni particles on the surface of support as shown in Figure 4.3 (e), resulting in the poor catalytic activity. On the other hand, the presence of Ag species in 1.5Ag1.5Zr/HZSM-5 catalyst significantly enhanced the light olefins selectivity, especially for ethylene and propylene. Moreover, C_5^+ products selectivity dramatically decreased. Among the catalysts tested, the 1.5Ag1.5Zr/HZSM-5 catalyst exhibited the highest light olefins yield which was 52.64 %wt. when compared to the other catalysts. This could be due to the high dehydrogenation activity of Ag species for this reaction. Furthermore, the results could be explained from the acid property of 1.5Ag1.5Zr/HZSM-5 catalyst. As shown in Table 4.2, the 1.5Ag1.5Zr/HZSM-5 catalyst provided the lowest total acid site when compared to other modified HZSM-5 catalysts, particularly for the decrease of strong acid site that can suppressed the production of aromatic and coke (Gao *et al.*, 2016). This can be concluded that the *n*-pentane catalytic cracking reaction is more favorable from the catalysts that provide low total acid site and lowest strong acid site in particular.



242044977

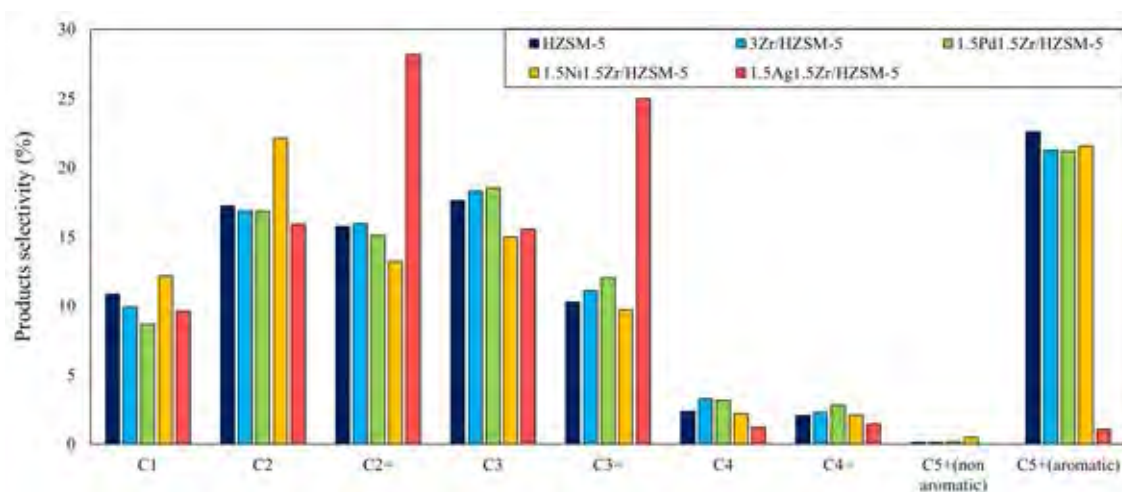


Figure 4.7 Products distribution from HZSM-5 and modified HZSM-5 catalysts.

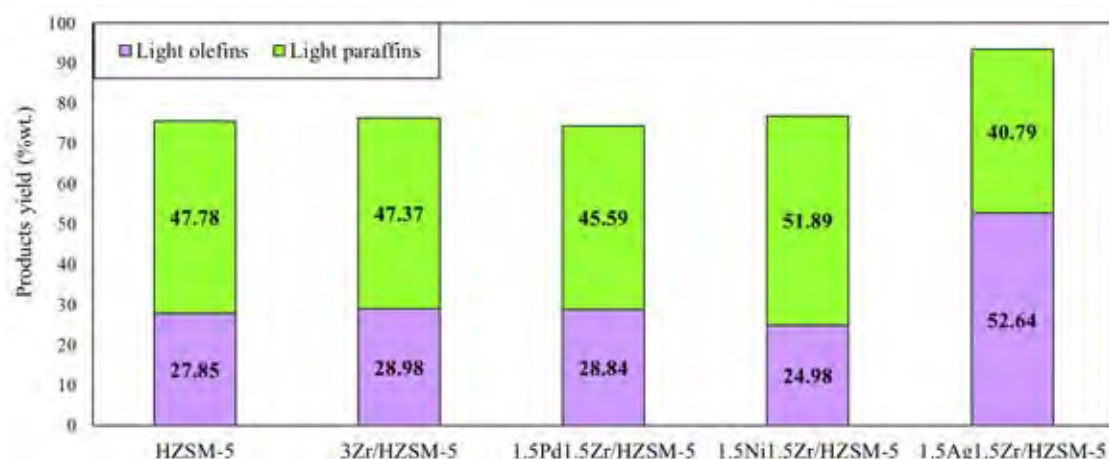


Figure 4.8 Products yield of light olefins and light paraffins from HZSM-5 and modified HZSM-5 catalysts.

The results of ethylene selectivity, propylene selectivity and propylene to ethylene ratio of HZSM-5 and modified HZSM-5 catalysts are shown in Figure 4.9. The HZSM-5 and modified HZSM-5 catalysts demonstrate the same results that the propylene selectivity is lower than ethylene selectivity. However, the 1.5Ag1.5Zr/HZSM-5 catalyst exhibited ethylene and propylene selectivity almost 2 times higher than other catalysts and reaches highest propylene to ethylene ratio of 0.89.

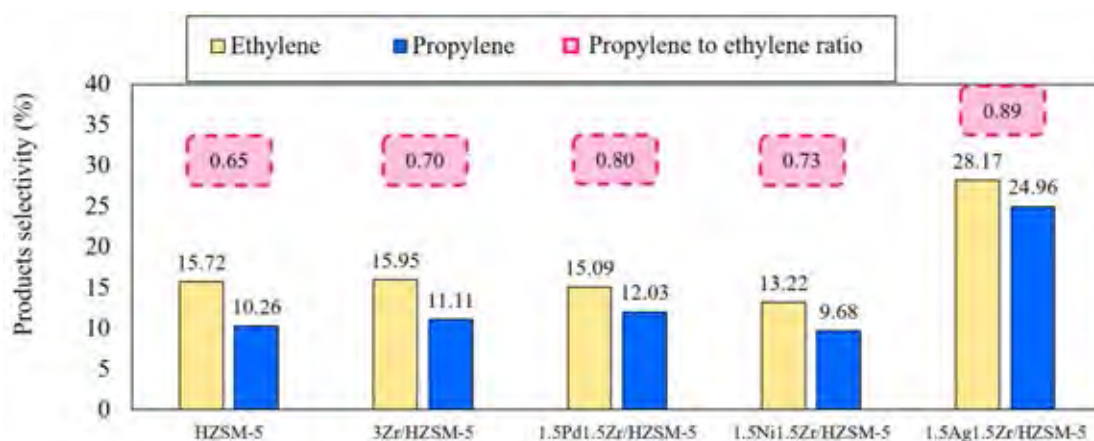


Figure 4.9 Ethylene selectivity, propylene selectivity and propylene to ethylene ratio from HZSM-5 and modified HZSM-5 catalysts.

To find the catalyst that could enhance the propylene to ethylene ratio beyond one, the 1.5Ag1.5Zr/HZSM-5 catalyst with various support $\text{SiO}_2/\text{Al}_2\text{O}_3$ ratios were further investigated.

4.2.2 Effect of HZSM-5 Zeolites $\text{SiO}_2/\text{Al}_2\text{O}_3$ Ratio

The 1.5Ag1.5Zr/HZSM-5 catalysts with different $\text{SiO}_2/\text{Al}_2\text{O}_3$ ratios of 23, 50 and 80 were performed in *n*-pentane catalytic cracking in order to investigate the effect of $\text{SiO}_2/\text{Al}_2\text{O}_3$ ratio to ethylene and propylene production. All of the results take a consider at time on stream (TOS) 3 h because the results from TOS 3 h show stable catalytic activity.

The product distribution from 1.5Ag1.5Zr/HZSM-5 catalysts with different $\text{SiO}_2/\text{Al}_2\text{O}_3$ ratios of 23, 50 and 80 are shown in Figure 4.10. It was found that the increasing of $\text{SiO}_2/\text{Al}_2\text{O}_3$ ratio decreased the methane and ethylene selectivity, increased the propylene and butenes selectivity. For propylene selectivity, 1.5Ag1.5Zr/HZSM-5 catalyst with $\text{SiO}_2/\text{Al}_2\text{O}_3$ ratio 80 exhibits the highest selectivity. This could be related to the high surface area, high pore volume and low acid property of 1.5Ag1.5Zr/HZSM-5 catalyst with different $\text{SiO}_2/\text{Al}_2\text{O}_3$ ratios of 23, 50 and 80 that are shown in Tables 4.1 and 4.2.

In terms of physical properties of catalysts, the 1.5Ag1.5Zr/HZSM-5 with different $\text{SiO}_2/\text{Al}_2\text{O}_3$ ratio have a high total surface area and pore volume. This could possibly enhance the adsorption of reactant on the catalyst surface and promote the light olefins and light paraffins production.

In terms of chemical properties of catalysts, the increase of $\text{SiO}_2/\text{Al}_2\text{O}_3$ ratio remarkably decreased the total acid site of the catalysts, including the amount of weak acid site and strong acid site. This could be illustrated that the lower amount of acid site catalyst is more preferable for propylene production.

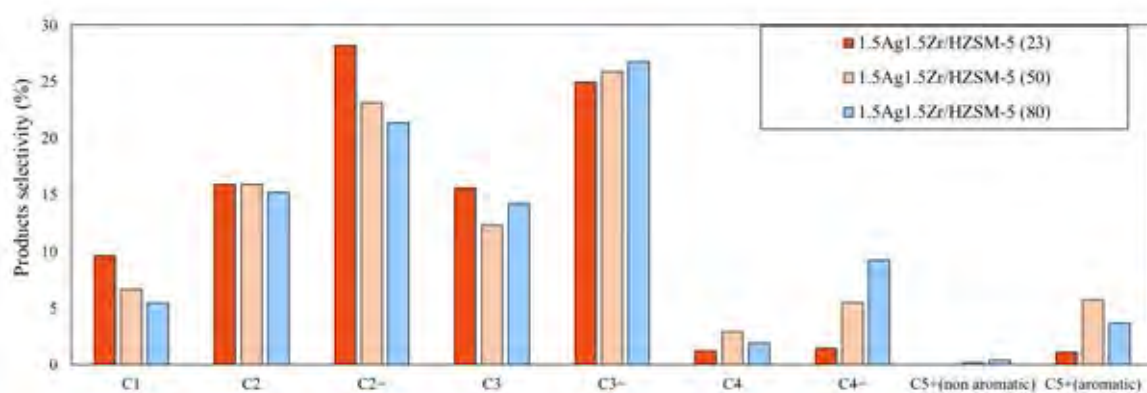


Figure 4.10 Products distribution from 1.5Ag1.5Zr/HZSM-5 catalysts with different $\text{SiO}_2/\text{Al}_2\text{O}_3$ ratios.

The light olefins and light paraffins yield from 1.5Ag1.5Zr/HZSM-5 catalysts with different $\text{SiO}_2/\text{Al}_2\text{O}_3$ ratios of 23, 50 and 80 are shown in Figure 4.11.

The results showed that 1.5Ag1.5Zr/HZSM-5 catalyst with $\text{SiO}_2/\text{Al}_2\text{O}_3$ ratio of 23 provided the highest yield of light olefins compared to other $\text{SiO}_2/\text{Al}_2\text{O}_3$ ratios catalysts. This could be ascribed to the highest conversion obtained from 1.5Ag1.5Zr/HZSM-5 catalyst with $\text{SiO}_2/\text{Al}_2\text{O}_3$ ratio of 23 which is 96.48%.

On the other hand, 1.5Ag1.5Zr/HZSM-5 catalyst with $\text{SiO}_2/\text{Al}_2\text{O}_3$ ratio of 80 provided the lowest light olefins and light paraffins yield due to its lowest conversion which is 77.55%. This can be concluded that the 1.5Ag1.5Zr/HZSM-5 catalyst with $\text{SiO}_2/\text{Al}_2\text{O}_3$ ratio of 23 shows a good performance in *n*-pentane catalytic cracking compared to other $\text{SiO}_2/\text{Al}_2\text{O}_3$ ratio catalysts.

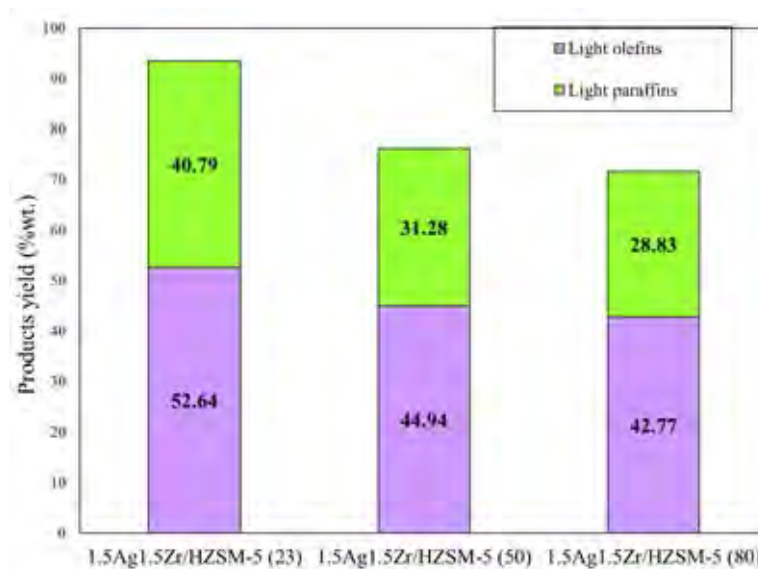


Figure 4.11 Products yield of light olefins and light paraffins from 1.5Ag1.5Zr/HZSM-5 catalysts with different SiO₂/Al₂O₃ ratios.

For the ethylene selectivity, propylene selectivity and propylene to ethylene ratio that obtained from 1.5Ag1.5Zr/HZSM-5 catalysts with different SiO₂/Al₂O₃ ratios of 23, 50 and 80 are shown in Figure 4.12.

The higher propylene selectivity as compared to ethylene selectivity observed on the 1.5Ag1.5Zr/HZSM-5 catalysts with SiO₂/Al₂O₃ ratios of 50 and 80 that achieved propylene selectivity 2.77% and 5.42% higher than ethylene selectivity. Besides, the obtained propylene to ethylene ratio from 1.5Ag1.5Zr/HZSM-5 catalyst increased with the increase of SiO₂/Al₂O₃ ratios. Particularly for the 1.5Ag1.5Zr/HZSM-5 catalyst with SiO₂/Al₂O₃ ratios 80 that provided the highest propylene to ethylene ratio of 1.25. This can be summarized that lower amount of total acid site in catalysts promoted the propylene selectivity.

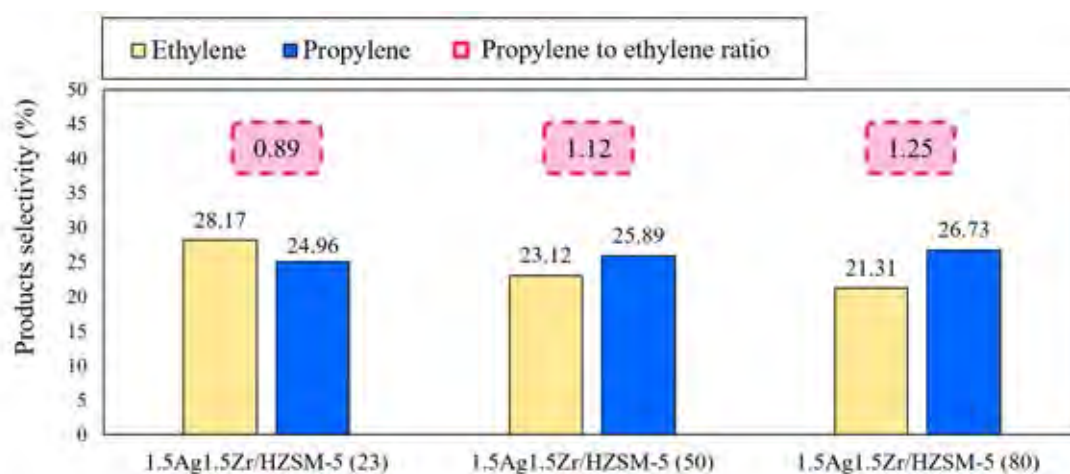


Figure 4.12 Ethylene selectivity, propylene selectivity and propylene to ethylene ratio from 1.5Ag1.5Zr/HZSM-5 catalysts with different SiO₂/Al₂O₃ ratios.

4.2.2.1 Effect of Weight Hourly Space Velocity (WHSV)

In order to investigate the dehydrogenation activity from second metal which is silver (Ag) on Zr/HZSM-5, the varying of WHSV 5 h⁻¹, 7 h⁻¹ and 9 h⁻¹ need to be observed. The WHSV determines the contact time between the reactant and the catalyst, the higher WHSV gives less contact time that can be minimized the side reaction and possibly enhanced the ethylene, propylene and butenes selectivity which are the products for examining the effect of dehydrogenation reaction in *n*-pentane cracking (Arjah *et al.*, 2017). Three WHSVs were tested 5 h⁻¹, 7 h⁻¹ and 9 h⁻¹ equivalent to a nitrogen flow of 30, 42 and 54 mL/min using 1.5Ag1.5Zr/HZSM-5 with SiO₂/Al₂O₃ ratio of 80 at temperature of 550 °C. The results at 3 h time on steam are given in Figure 4.13, at higher WHSV, the conversion was decreased from 77.55%, 66.09% and 55.46%, respectively. For the product distribution, the selectivity of ethylene, propylene and butenes increased when increase WHSV, while the selectivity of methane, ethane, propane, butanes and C₅⁺ products (including non-aromatic and aromatic) decreased when increase WHSV. The observed results confirm that silver site helps to promote the dehydrogenation activity leadings to higher olefins production. Moreover, the increase of WHSV can be minimized the undesired products from side reaction which are C₅⁺ products (including non-aromatic and aromatic) that occurred from longer contact time.

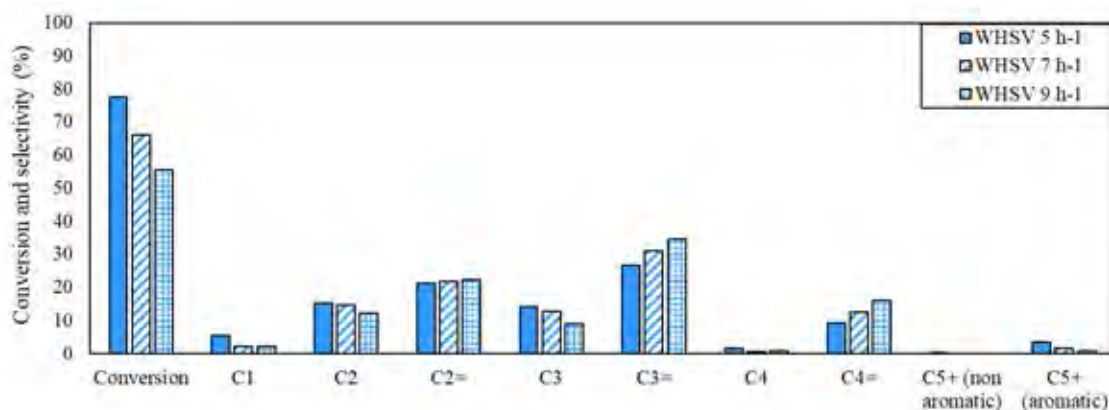


Figure 4.13 Effect of WHSV on conversion and product distribution from 1.5Ag1.5Zr/HZSM-5 catalyst with SiO₂/Al₂O₃ ratio of 80 at TOS 3 h.

In addition, in Figure 4.14 showed that the increase of WHSV enhances the propylene to ethylene ratio, especially for WHSV 9 h⁻¹ that exhibits the highest propylene to ethylene ratio equals to 1.54.

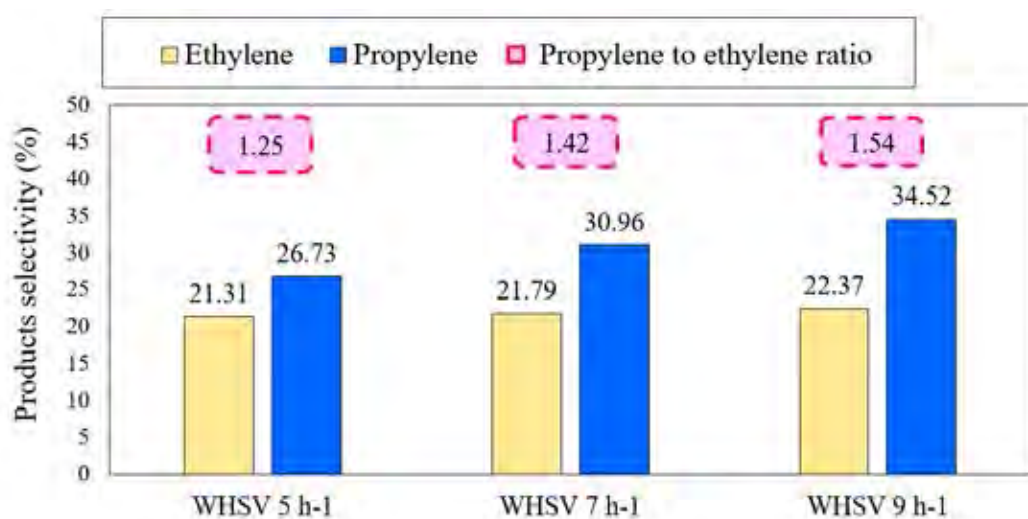


Figure 4.14 Effect of WHSV on ethylene, propylene selectivity and propylene to ethylene ratio from 1.5Ag1.5Zr/HZSM-5 catalyst with SiO₂/Al₂O₃ ratio of 80 at TOS 3 h.

4.3 Catalytic Stability

The catalytic stability was performed at 550 °C under atmospheric pressure with *n*-pentane WHSV of 5 h⁻¹ and maintained the reaction for 5 h.

4.3.1 Effect of Second Metal Loadings

The obtained conversion and light olefins selectivity, ethylene selectivity and propylene selectivity as a function of time on stream (TOS) are shown in Figures 4.15, 4.16, 4.17 and 4.18, respectively.

The HZSM-5 and modified HZSM-5 catalysts exhibited high conversion ranging from 94.8% to 99.9% and maintained the good stability even after a long time except for 1.5Ni1.5Zr/HZSM-5 catalyst. The conversion of 1.5Ni1.5Zr/HZSM-5 catalyst is decreased after 3 h, corresponding to the result from TPO and CHNS elemental analyzer that the spent 1.5Ni1.5Zr/HZSM-5 catalyst had the highest coke deposition. This can be concluded that 1.5Ni1.5Zr/HZSM-5 catalyst cannot provide a good stability.

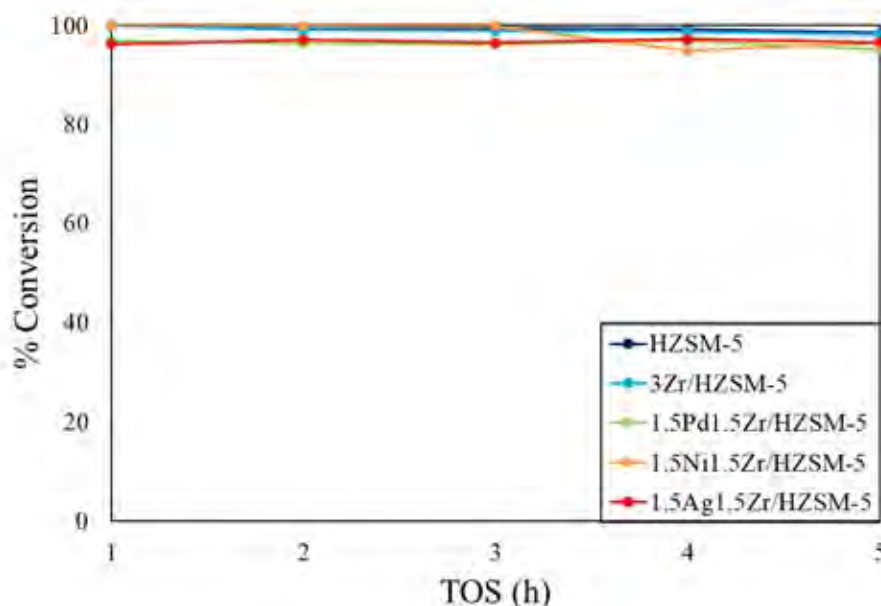


Figure 4.15 Conversion of *n*-pentane over HZSM-5 and modified HZSM-5 catalysts at 550 °C, atm, WHSV of 5 h⁻¹ as a function of time on stream (TOS).

The results of light olefins selectivity, ethylene selectivity and propylene selectivity from HZSM-5 and modified HZSM-5 catalysts indicated the similar results. 1.5Ag1.5Zr/HZSM-5 catalyst provided the highest light olefins selectivity, ethylene selectivity and propylene selectivity as compared to the parent HZSM-5 and other modified HZSM-5 catalysts. Moreover, this catalyst also maintained a good stability after 5 h, consistent with the lowest in coke formation that investigated by TPO and CHNS elemental analyzer.

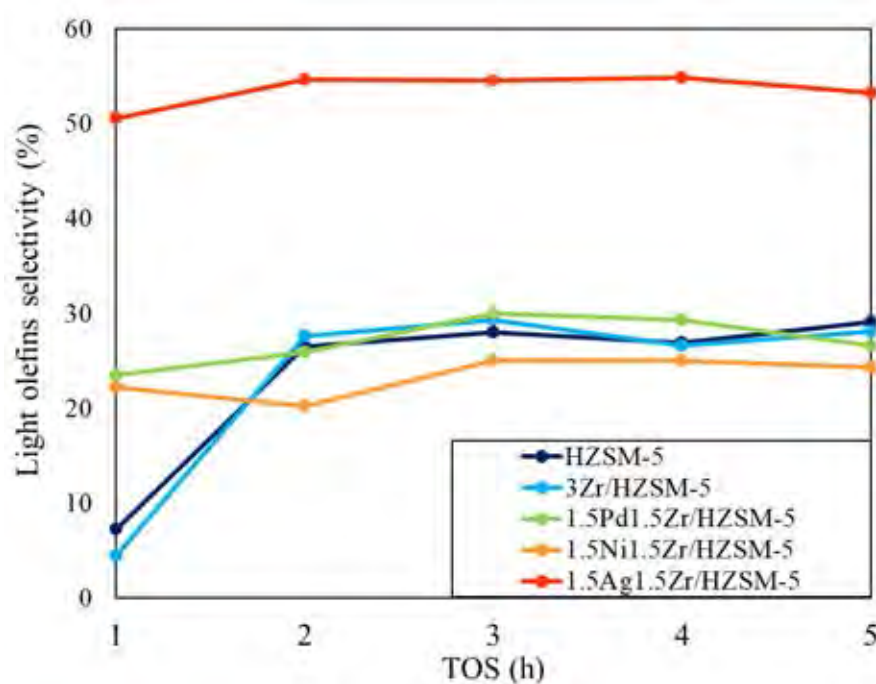


Figure 4.16 Light olefins selectivity over HZSM-5 and modified HZSM-5 catalysts at 550 °C, atm, WHSV of 5 h⁻¹ as a function of time on stream (TOS).

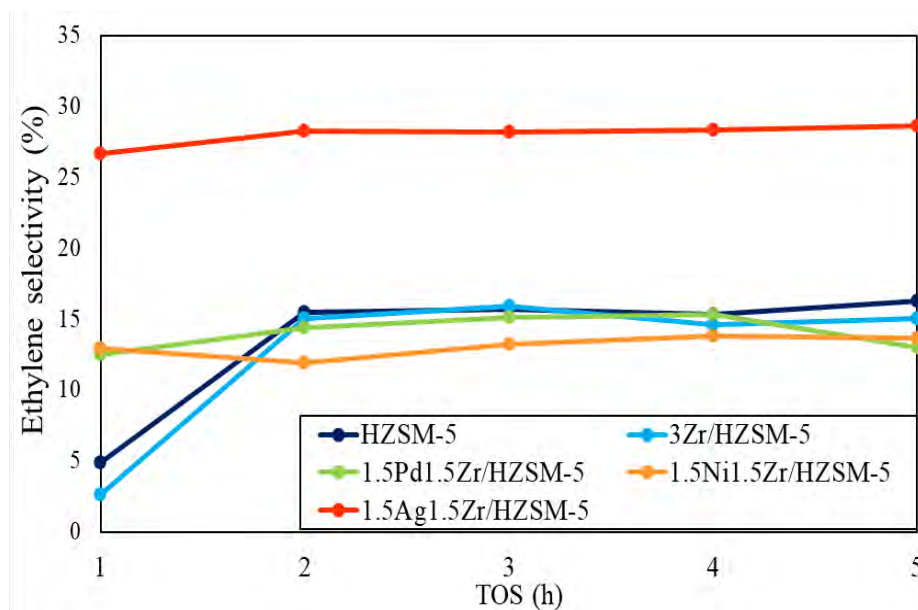


Figure 4.17 Ethylene selectivity of HZSM-5 and modified HZSM-5 catalysts at 550 °C, atm, WHSV of 5 h⁻¹ as a function of time on stream (TOS).

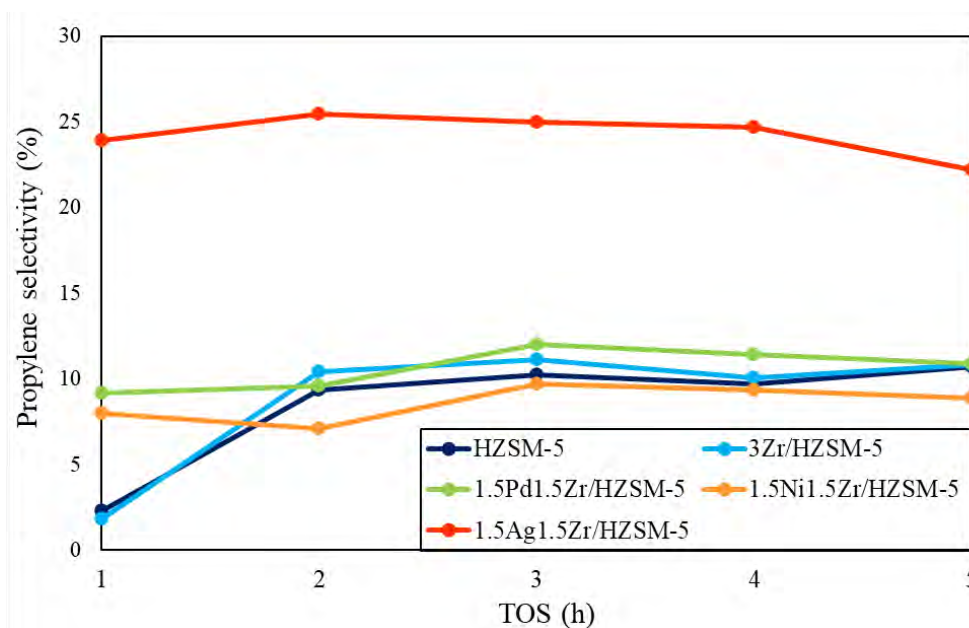


Figure 4.18 Propylene selectivity of HZSM-5 and modified HZSM-5 catalysts at 550 °C, atm, WHSV of 5 h⁻¹ as a function of time on stream (TOS).

4.3.2 Effect of SiO₂/Al₂O₃ Ratios

The obtained conversion over 1.5Ag1.5Zr/HZSM-5 catalysts with different SiO₂/Al₂O₃ ratios of 23, 50 and 80 are shown in Figure 4.19. It was obviously found that 1.5Ag1.5Zr/HZSM-5 catalyst with SiO₂/Al₂O₃ ratio of 23 provided the best stability as compared to other catalysts. Meanwhile, 1.5Ag1.5Zr/HZSM-5 catalyst with SiO₂/Al₂O₃ ratio of 80 gives the worst stability which dramatically decreased to 68.3% after 5 h.

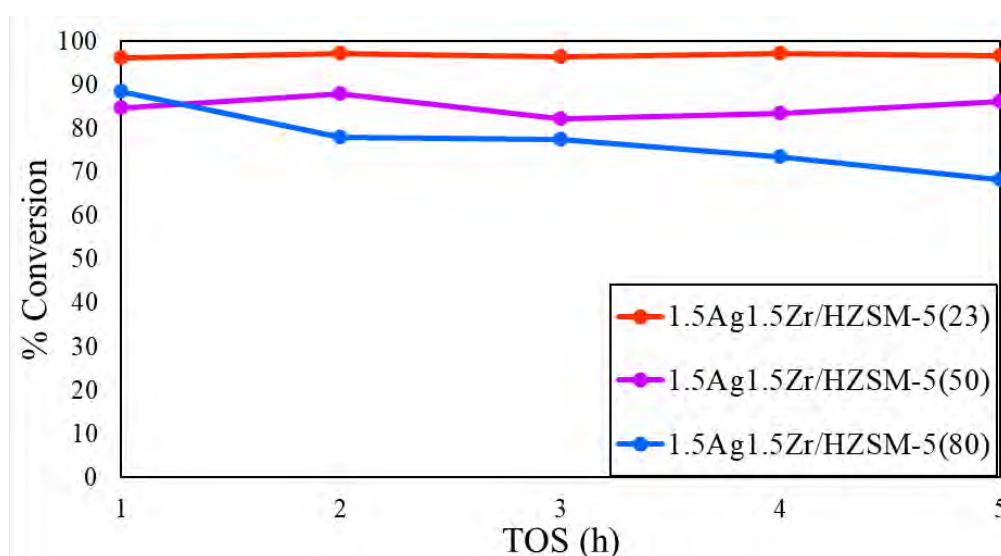


Figure 4.19 Conversion of *n*-pentane over 1.5Ag1.5Zr/HZSM-5 catalysts with different SiO₂/Al₂O₃ ratios at 550 °C, atm, WHSV of 5 h⁻¹ as a function of time on stream (TOS).

The light olefins selectivity of 1.5Ag1.5Zr/HZSM-5 catalysts with different SiO₂/Al₂O₃ ratios of 23, 50 and 80 are shown in Figure 4.20. The results showed that 1.5Ag1.5Zr/HZSM-5 (80) exhibited low light olefins selectivity at first hour then increased in 2 h and maintained the highest light olefins selectivity. On the other hand, 1.5Ag1.5Zr/HZSM-5 (50) exhibited the highest light olefins selectivity which is 57.1% at first hour, then decreased to 46.3% in after 5 h.

For 1.5Ag1.5Zr/HZSM-5 (23), it did not significantly change in light olefins selectivity after 5 h. It provided 50.6% at first hour, then increased to 53.3% after 5 h.

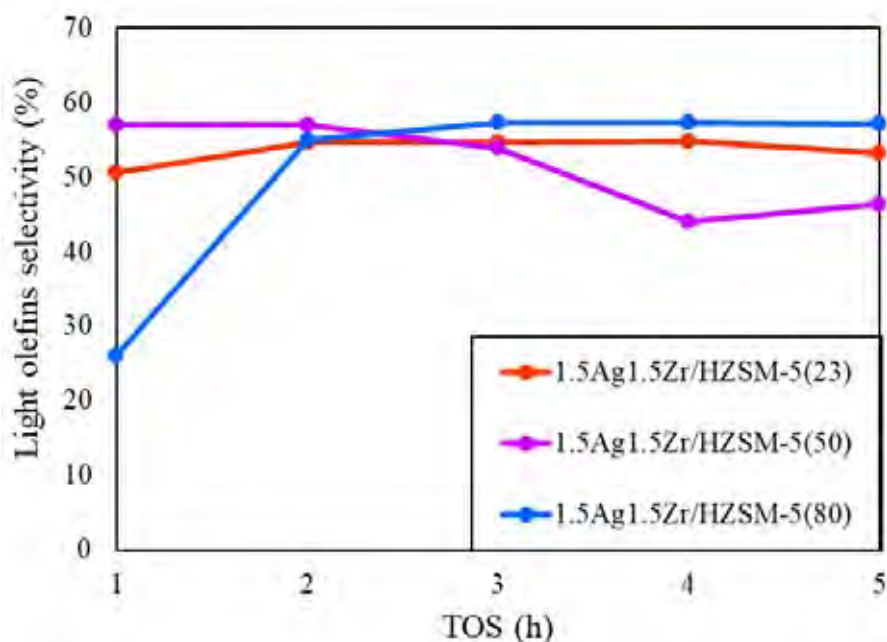


Figure 4.20 Light olefins selectivity of 1.5Ag1.5Zr/HZSM-5 catalysts with different SiO₂/Al₂O₃ ratios at 550 °C, atm, WHSV of 5 h⁻¹ as a function of time on stream (TOS).

The results of ethylene selectivity and propylene selectivity from 1.5Ag1.5Zr/HZSM-5 catalysts with different SiO₂/Al₂O₃ ratios are shown in Figures 4.21 and 4.22, respectively. For ethylene selectivity, 1.5Ag1.5Zr/HZSM-5 (23) gave the highest ethylene selectivity which is 26.7% at first hour, then slightly increased to 28.6% after 5 h. The 1.5Ag1.5Zr/HZSM-5 (80) gave the lowest selectivity which is 8.9% at first hour, then increased to 21.3% after 5 h. On the contrary, 1.5Ag1.5Zr/HZSM-5 (50) gave the ethylene selectivity 24.4% at first hour, then slightly decreased to 21.0% after 5 h. In terms of propylene selectivity as a function of TOS, 1.5Ag1.5Zr/HZSM-5 (50) and 1.5Ag1.5Zr/HZSM-5 (80) give the similar result as show in ethylene selectivity as a function of TOS.

The 1.5Ag1.5Zr/HZSM-5 (80) provided the highest propylene selectivity which was 26.5% after 5 h. In opposition, 1.5Ag1.5Zr/HZSM-5 (50) showed the lowest propylene selectivity which was 19.4% after 5 h.

For 1.5Ag1.5Zr/HZSM-5 (23), it seems to have a good stability which provided the highest level of conversion at first (96.3%) and maintained the

highest conversion (96.6%) after 5 h. However, the 1.5Ag1.5Zr/HZSM-5 (23) cannot reached the highest propylene selectivity as expected while the 1.5Ag1.5Zr/HZSM-5 (80) can reached (26.5%).

In the considering of catalyst stability, 1.5Ag1.5Zr/HZSM-5 (23) exhibited the highest stability after a long time of reaction. On the other hand, with the ratio of $\text{SiO}_2/\text{Al}_2\text{O}_3$ further increased, the catalytic conversion slightly decreased. This could be due to the acidity of catalysts that higher $\text{SiO}_2/\text{Al}_2\text{O}_3$ ratio of the support exhibited lower acidity of catalysts, resulting quick deactivation of catalysts that was observed from the amount of lower coke formation from higher $\text{SiO}_2/\text{Al}_2\text{O}_3$ ratio due to the lower activity (Nawaz *et al.*, 2010).

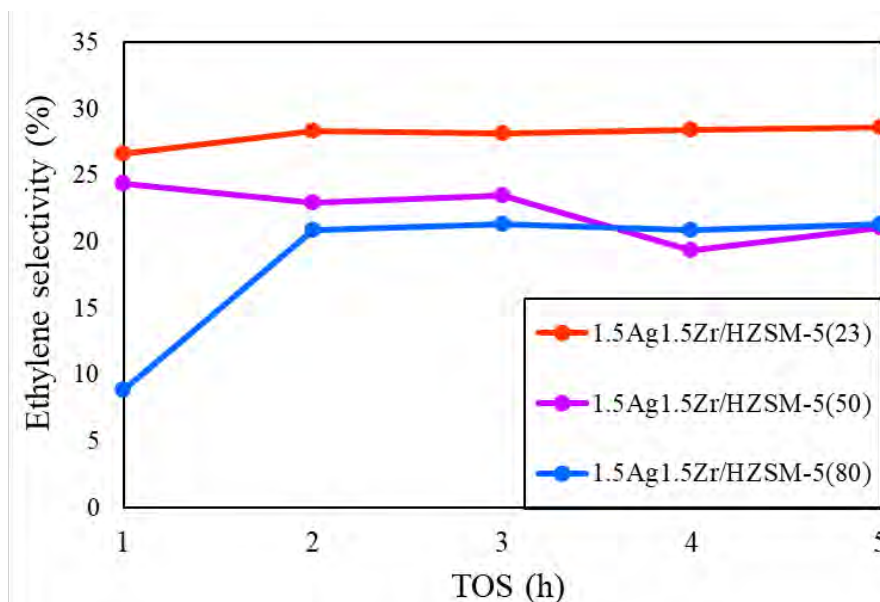


Figure 4.21 Ethylene selectivity of 1.5Ag1.5Zr/HZSM-5 catalysts with different $\text{SiO}_2/\text{Al}_2\text{O}_3$ ratios at 550 °C, atm, WHSV of 5 h⁻¹ as a function of time on stream (TOS).

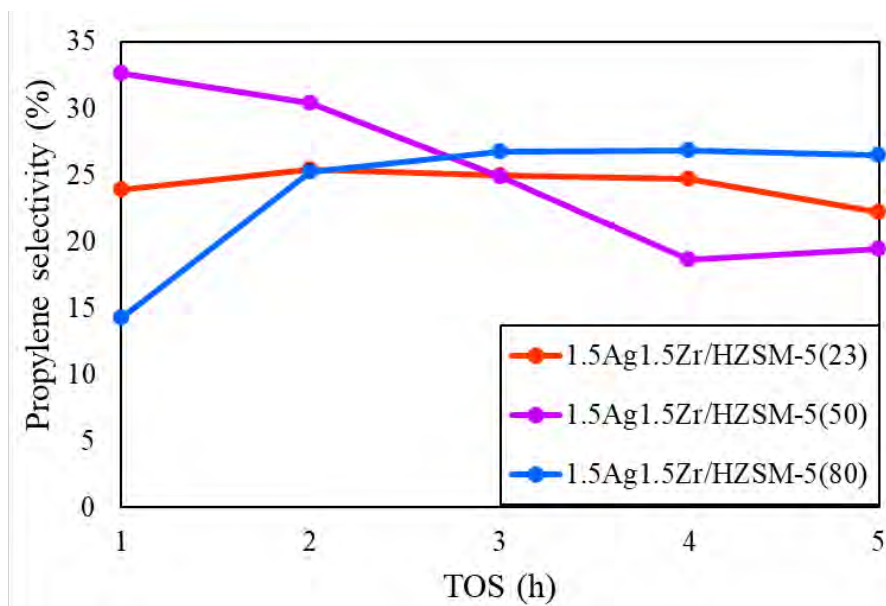


Figure 4.22 Propylene selectivity of 1.5Ag1.5Zr/HZSM-5 catalysts with different SiO₂/Al₂O₃ ratios at 550 °C, atm, WHSV of 5 h⁻¹ as a function of time on stream (TOS).

CHAPTER 5

CONCLUSIONS AND RECOMMENDATIONS

5.1 Conclusions

In order to improve the hybrid catalysts that can be enhanced the light olefins production and propylene to ethylene ratio for the conversion of *n*-pentane catalytic cracking, this work was divided into two major scopes. In the first scope, the effect of second metals on Zr/HZSM-5 catalysts were studied using Pd, Ni and Ag species which has the expectation to improve dehydrogenation activity of the catalysts. It was found that the addition of Ag into Zr/HZSM-5 catalyst was significantly affected the light olefins production, especially for ethylene and propylene selectivity. The 1.5Ag1.5Zr/HZSM-5 catalyst exhibited the highest light olefins yield, ethylene selectivity and propylene selectivity which is 54.6 %wt., 28.2 % and 25.0 %, respectively (at TOS 3 h). The results could be related to the acid properties of catalysts that the addition of Ag species decreased the amount of total acid site, resulted in the lowest acidity catalyst, while other second metals addition increased the amount of total acid site, particularly for the strong acid site. To gain more understanding, the second scope which is studied the effect of HZSM-5 SiO₂/Al₂O₃ ratio on 1.5Ag1.5Zr/HZSM-5 catalysts. The 1.5Ag1.5Zr/HZSM-5 catalysts with different SiO₂/Al₂O₃ ratio 23, 50 and 80 showed different light olefins yield, product selectivity and acidity. The highest light olefins yield came from 1.5Ag1.5Zr/HZSM-5 (23) catalyst presented at 52.6%, followed by 1.5Ag1.5Zr/HZSM-5 (50) 44.9%, and 1.5Ag1.5Zr/HZSM-5 (80). catalyst 42.8%. In terms of product selectivity, the 1.5Ag1.5Zr/HZSM-5 (80) catalyst gave the highest propylene selectivity, while lowest ethylene selectivity. This could be due to the lowest amount of total acid site from 1.5Ag1.5Zr/HZSM-5 (80) catalyst which preferable in propylene production. However, the 1.5Ag1.5Zr/HZSM-5 (23) catalyst seemed to be the best performance catalyst due to its high light olefins production and high level of conversion. In conclusion, the appropriated catalyst for *n*-pentane catalytic cracking with the aim of promote light olefins yield and propylene to ethylene ratio (>1) should have optimum acidity and good dehydrogenation activity.

5.2 Recommendations

To obtain more understanding about the effect of acidity from modified HZSM-5 catalysts, especially hybrid AgZr/HZSM-5 catalyst on *n*-pentane catalytic cracking, Brønsted acid site and Lewis acid site need to be investigated using FTIR-pyridine. Moreover, in order to explain more about the metal dispersion on HZSM-5 support which could probably affected to the catalytic cracking reaction, the exactly location and species of metal oxides need to be considered, determining by EDS mapping.



242044977

CU IThesis 6171002063 thesis / recv: 31072563 03:53:59 / seq: 17

APPENDICES

Appendix A Calculation of Activity Testing

Calculation of *n*-pentane feed flow rate at $WHSV = 5 \text{ h}^{-1}$

Amount of HZSM-5 catalyst = 0.20 g

$$WHSV = \frac{\text{Flow rate } (\frac{g}{h})}{\text{Weight of catalyst } (g)}$$

$$5 \text{ h}^{-1} = \frac{\text{Flow rate } (\frac{g}{h})}{0.20 \text{ g}}$$

$$\text{Flow rate} = 1.0 \text{ g/h}$$

According to *n*-pentane density which is equal to 0.626 g/mL at 20 °C, 1 atm

$$\text{Flow rate} = \frac{1.0 \text{ g/h}}{0.626 \text{ g/mL}} = 1.597 \text{ mL/h}$$

REFERENCES

- Alotaibi, F.M., González-Cortés, S., Alotibi, M.F., Xiao, T., Al-Megren, H., Yang, G., and Edwards, P.P. (2018). Enhancing the production of light olefins from heavy crude oils: Turning challenges into opportunities. Catalysis Today, 317, 86-98.
- Amghizar, I., Vandewalle, L.A., Van Geem, K.M., and Marin, G.B. (2017). New Trends in Olefin Production. Engineering, 3(2), 171-178.
- Arjah, A., Albahar, M., Li, C., and Garforth, A. (2017). Selective Cracking of Light Olefins to Ethene and Propene. Chemical Engineering Transactions, 57, 883-888.
- Diao, Z., Wang, L., Zhang, X., and Liu, G. (2015). Catalytic cracking of supercritical n-dodecane over meso-HZSM-5@Al-MCM-41 zeolites. Chemical Engineering Science, 135, 452-460.
- Gao, Y., Zheng, B., Wu, G., Ma, F., and Liu, C. (2016). Effect of the Si/Al ratio on the performance of hierarchical ZSM-5 zeolites for methanol aromatization. RSC Advances, 6(87), 83581-83588.
- Haribal, V.P., Chen, Y., Neal, L., and Li, F. (2018). Intensification of Ethylene Production from Naphtha via a Redox Oxy-Cracking Scheme: Process Simulations and Analysis. Engineering, 4(5), 714-721.
- He, C., Li, P., Cheng, J., Wang, H., Li, J., Li, Q., and Hao, Z. (2010). Synthesis and characterization of Pd/ZSM-5/MCM-48 biporous catalysts with superior activity for benzene oxidation. Applied Catalysis A: General, 382(2), 167-175.
- Hou, X., Qiu, Y., Tian, Y., Diao, Z., Zhang, X., and Liu, G. (2018). Reaction pathways of n-pentane cracking on the fresh and regenerated Sr, Zr and La-loaded ZSM-5 zeolites. Chemical Engineering Journal, 349, 297-308.
- Hou, X., Qiu, Y., Zhang, X., and Liu, G. (2017). Effects of regeneration of ZSM-5 based catalysts on light olefins production in n-pentane catalytic cracking. Chemical Engineering Journal, 321, 572-583.
- Hou, X., Zhu, W., Tian, Y., Qiu, Y., Diao, Z., Feng, F., Zhang, X., and Liu, G. (2019). Superiority of ZrO₂ surface enrichment on ZSM-5 zeolites in n-pentane catalytic cracking to produce light olefins. Microporous and Mesoporous Materials, 276,

41-51.

- Jodaei, A., Salari, D., Niaei, A., Khatamian, M., and Hosseini, S.A. (2011). Oxidation of ethyl acetate by a high performance nanostructure (Ni, Mn)-Ag/ZSM-5 bimetallic catalysts and development of an artificial neural networks predictive modeling. J Environ Sci Health A Tox Hazard Subst Environ Eng, 46(1), 50-62.
- Kee, R.J., Karakaya, C., and Zhu, H. (2017). Process intensification in the catalytic conversion of natural gas to fuels and chemicals. Proceedings of the Combustion Institute, 36(1), 51-76.
- Kubo, K., Iida, H., Namba, S., and Igarashi, A. (2015). Comparison of steaming stability of Cu-ZSM-5 with those of Ag-ZSM-5, P/H-ZSM-5, and H-ZSM-5 zeolites as naphtha cracking catalysts to produce light olefin at high temperatures. Applied Catalysis A: General, 489, 272-279.
- Le Van Mao, R., Muntasar, A., Yan, H.T., and Zhao, Q. (2009). Catalytic Cracking of Heavy Olefins into Propylene, Ethylene and Other Light Olefins. Catalysis Letters, 130(1-2), 86-92.
- Lee, J., Ryou, Y., Cho, S.J., Lee, H., Kim, C.H., and Kim, D.H. (2018). Investigation of the active sites and optimum Pd/Al of Pd/ZSM-5 passive NO adsorbers for the cold-start application: Evidence of isolated-Pd species obtained after a high-temperature thermal treatment. Applied Catalysis B: Environmental, 226, 71-82.
- Maia, A.J., Louis, B., Lam, Y.L., and Pereira, M.M. (2010). Ni-ZSM-5 catalysts: Detailed characterization of metal sites for proper catalyst design. Journal of Catalysis, 269(1), 103-109.
- Maia, A.J., Oliveira, B.G., Esteves, P.M., Louis, B., Lam, Y.L., and Pereira, M.M. (2011). Isobutane and n-butane cracking on Ni-ZSM-5 catalyst: Effect on light olefin formation. Applied Catalysis A: General.
- Nawaz, Z., Qing, S., Jixian, G., Tang, X., and Wei, F. (2010). Effect of Si/Al ratio on performance of Pt-Sn-based catalyst supported on ZSM-5 zeolite for n-butane conversion to light olefins. Journal of Industrial and Engineering Chemistry, 16(1), 57-62.
- Ono, Y., and Baba, T. (2015). Unique properties of silver cations in solid-acid catalysis by zeolites and heteropolyacids. Phys Chem Chem Phys, 17(24), 15637-15654.

- Plotkin, J.S. (2015). The propylene gap: how can it be filled. Washington, DC: American Chemical Society. Accessed December, 1, 2018.
- Popova, M., Djinovic, P., Ristic, A., Lazarova, H., Drazic, G., Pintar, A., Balu, A.M., and Novak Tusar, N. (2018). Vapor-Phase Hydrogenation of Levulinic Acid to gamma-Valerolactone Over Bi-Functional Ni/HZSM-5 Catalyst. Front Chem, 6, 285.
- Resasco, D.E., Marcus, B.K., Huang, C.S., and Durante, V.A. (1994). Isobutane dehydrogenation over sulfided nickel catalysts. Journal of Catalysis, 146(1), 40-55.
- Shirazi, L., Jamshidi, E., and Ghasemi, M.R. (2008). The effect of Si/Al ratio of ZSM-5 zeolite on its morphology, acidity and crystal size. Crystal Research and Technology, 43(12), 1300-1306.
- Silva, L.S.d., Araki, C.A., Marcucci, S.M.P., Silva, V.L.d.S.T.d., and Arroyo, P.A. (2019). Desilication of ZSM-5 and ZSM-12 Zeolites with Different Crystal Sizes: Effect on Acidity and Mesoporous Initiation. Materials Research, 22(2).
- Usman, A., Siddiqui, M.A.B., Hussain, A., Aitani, A., and Al-Khattaf, S. (2017). Catalytic cracking of crude oil to light olefins and naphtha: Experimental and kinetic modeling. Chemical Engineering Research and Design, 120, 121-137.
- Wang, Q., Zhu, M., Zhang, H., Xu, C., Dai, B., and Zhang, J. (2019). Enhanced catalytic performance of Zr-modified ZSM-5-supported Zn for the hydration of acetylene to acetaldehyde. Catalysis Communications, 120, 33-37.
- Weng, Y., Qiu, S., Ma, L., Liu, Q., Ding, M., Zhang, Q., Zhang, Q., and Wang, T. (2015). Jet-Fuel Range Hydrocarbons from Biomass-Derived Sorbitol over Ni-HZSM-5/SBA-15 Catalyst. Catalysts, 5(4), 2147-2160.
- Wu, Z., Wegener, E.C., Tseng, H.-T., Gallagher, J.R., Harris, J.W., Diaz, R.E., Ren, Y., Ribeiro, F.H., and Miller, J.T. (2016). Pd-In intermetallic alloy nanoparticles: highly selective ethane dehydrogenation catalysts. Catalysis Science & Technology, 6(18), 6965-6976.
- Yang, M., Dong, Y., Fei, S., Ke, H., and Cheng, H. (2014). A comparative study of catalytic dehydrogenation of perhydro-N-ethylcarbazole over noble metal catalysts. International Journal of Hydrogen Energy, 39(33), 18976-18983.

- Zhang, J., Jiang, Q., Yang, D., Zhao, X., Dong, Y., and Liu, R. (2015). Reaction-activated palladium catalyst for dehydrogenation of substituted cyclohexanones to phenols and H₂ without oxidants and hydrogen acceptors. Chem Sci, 6(8), 4674-4680.
- Zimmermann, H., and Walzl, R. (2000). Ethylene. Ullmann's Encyclopedia of Industrial Chemistry.

VITA

NAME	Bharanabha Makkaroon
DATE OF BIRTH	16 Dec 1995
PLACE OF BIRTH	Nakhorn Ratchasima
INSTITUTIONS ATTENDED	Suranaree University of Technology
HOME ADDRESS	1841/50 Suebsiri Grandville, Soi Suebsiri35, Suebsiri road, Nai mueang sub district, Mueang District, Nakhorn Ratchasima 30000



242044977

CU IThesis 6171002063 thesis / recv: 31072563 03:53:59 / seq: 17